EUROPEAN ORGANIZATION FOR NUCLEAR RESEARCH

LEP EWWG / LS 2000-01
July 20, 2000

Combination procedure for the precise determination of Z–boson parameters from results of the LEP experiments

The LEP Collaborations, ALEPH, DELPHI, L3 and OPAL [1)] and
the Line Shape Sub-group of the LEP Electroweak Working Group [2)]

Abstract

The precise determination of the Z-boson parameters from the measurements at the Z resonance by the four collaborations ALEPH, DELPHI, L3 and OPAL in e^+e^- collisions at the large electron positron collider LEP at CERN is a landmark for precision tests of the electroweak theory. The four experiments measured quantities which were used to extract the mass and width of the Z-boson, the hadronic cross-section at the pole of the resonance, the ratio of hadronic and leptonic decay widths, and the leptonic forward-backward asymmetries at the pole. The combination procedure based on these parameters is presented in this paper.

Contributed Paper for ICHEP2000

[1)] The full list of authors may be found in References [1, 2, 3, 4]

[2)] The members of the line shape group are: G. Duckeck, M. Grünewald, T. Kawamoto, R. Kellogg, G. Martinez, J. Mnich, A. Olshevski, B. Pietrzyk, G. Quast, P. Renton, E. Tournefier

1 Introduction

Between the years 1989 and 1995 the e^+e^- collider LEP at CERN provided interactions at centre-of-mass energies, $\sqrt{s}$, ranging from 88 to 95 GeV, *i.e.*, around the mass of the Z boson (LEP I phase). An important aspect of physics at LEP concerns the analysis of fermion-pair production in e^+e^- collisions [5]. The four LEP experiments ALEPH [6], DELPHI [7], L3 [8] and OPAL [9] analysed, in particular, hadron (quark-pair) production and the pair production of charged leptons, $\ell = e, \mu, \tau$.

At various centre-of-mass energies, total cross-sections are measured for all processes, while forward-backward asymmetries are measured in lepton-pair production [1, 2, 3, 4]. These measurements of so-called *realistic observables* allow the determination of various properties of the Z boson, such as its mass, total and partial decay widths, and coupling constants to fermions (*pseudo-observables*). For the extraction of the pseudo-observables, the experiments perform model-independent fits to their measured realistic observables [1, 2, 3, 4].

To obtain the best possible precision the results of the four LEP experiments have to be averaged. A combination of realistic observables constitutes an extremely complicated task, as it involves hundreds of measurements, each with specific cuts and experimental errors which are correlated among different centre-of-mass energies and data taking periods and also among the LEP experiments. Therefore, the combination of the four LEP experiments is performed on the basis of the four sets of pseudo-observables. As will be shown here, this is possible without significant loss of precision.

This paper describes the combination procedure adopted by the LEP electroweak working group [10]. Additional fits to the experimental data, usually not contained in the individual publications quoted above, were provided by the experiments and are documented in this paper. A large effort is devoted to the treatment of systematic errors and their correlation among the LEP experiments, such that the combination procedure yields a correct and optimal estimator for the averages.

This paper is organised as follows: Sec. 2 summarises the information about the LEP I running relevant for this paper. Sec. 3 presents a brief introduction to the pseudo-observables used to parametrise the realistic observables around the Z resonance. The individual experimental results are presented in Sec. 4. Sources of correlated systematic errors between experiments and their effects on the pseudo-observables are discussed in Sec. 5. In Sec. 6, studies of various methods for combining the results are presented. The resulting pseudo-observables are then considered in the framework of a specific model, the minimal Standard Model (SM), and are compared with direct SM fits to the realistic observables. The conclusions are summarised in Sec. 7.

2 Z resonance scans at LEP I

Running of LEP in the years from 1989 to 1995 was dedicated to precision studies of the Z boson parameters. e^+e^- collisions were provided at several well-determined centre-of-mass

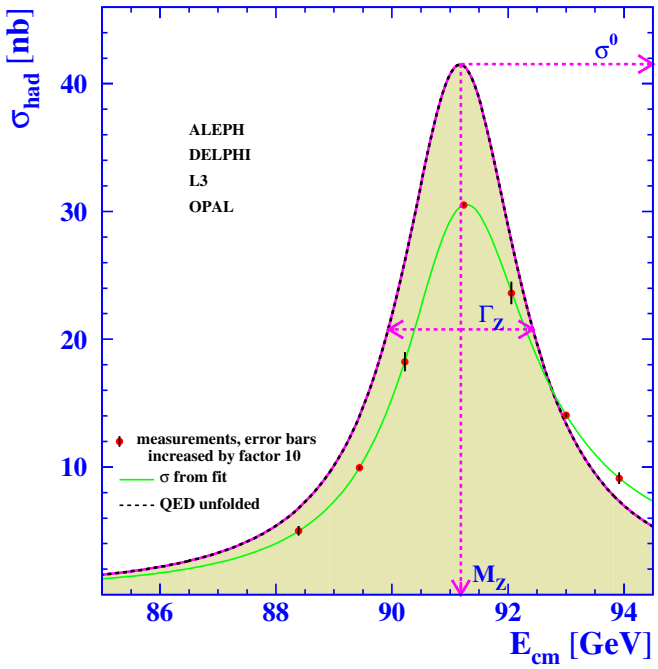

Figure 1: *Average over measurements of the hadronic cross-sections by the four experiments, as a function of centre-of-mass energy. The shaded curve shows the QED deconvoluted cross-section, which defines the* Z *parameters described in the text.*

energies around the Z resonance, with steadily increasing performance. The set of measurements collected by the experiments consists of the hadronic and leptonic cross-sections and the leptonic forward-backward asymmetries around seven points in centre-of-mass energy, over six years of running at LEP I. In addition, changes of experimental conditions, such as the inclusion of new detector components, made it necessary to subdivide the data samples even further. The full LEP I data set consists of about 4×200 individual cross-section and asymmetry measurements. From these each experiment has extracted a set of parameters describing the cross-section around the Z resonance, which include the mass, m_{Z}, and width, Γ_{Z}, of the Z and the total cross-section for $\mathrm{q\overline{q}}$ production, σ^o_{h}. These parameters are discussed in detail in Sec. 3 . QED corrections from photon radiation are large around the Z resonance due to the rapid variation of the cross-sections with centre-of-mass energy. For illustration, Fig. 1 shows the average over the hadronic cross-section measurements by the four experiments, together with the fitted line shape curve before and after unfolding photon radiation. The cross-section is almost completely dominated by on-shell Z production, although photon exchange and the $\gamma - \mathrm{Z}$ interference contribution are not negligible. The measurements are sensitive to higher-order electroweak corrections. These modify the tree-level couplings of the Z to fermions, and are quantified in terms of electroweak form

factors.

Much effort was dedicated to the precise determination of the energy of the colliding beams, which reached an absolute precision of about 20×10^{-6}. This level of precision is vital for the precision of the measurements of the mass and width of the Z. All the experiments replaced their first-generation luminosity detectors, which had precisions around the percent level, by high-precision devices capable of pushing systematic errors on the acceptance of small-angle Bhabha events below one per-mille. As a consequence of these improvements during LEP I running, statistical and systematic errors are much smaller for the last three years of data taking, which hence dominate the precision achieved on the Z parameters.

2.1 Event selection and statistics

The first Z bosons at LEP were produced and observed by the four experiments in summer 1989. Since then the operation of the machine and its performance had been steadily improved. At the end of data taking around the Z resonance in autumn 1995 the peak luminosity had reached nearly twice its design value. Tab. 1 summarises the data taking periods, the approximate centre-of-mass energies and the delivered integrated luminosities.

year	beam energy range [GeV]	integrated luminosity [pb^{-1}]
1989	[88.2 , 94.2]	1.4
1990	[88.2 , 94.2]	7.6
1991	[88.5 , 93.7]	17.3
1992	91.3	28.6
1993	89.4, 91.2, 93.0	40.0
1994	91.2	64.5
1995	89.4, 91.3, 93.0	39.8

Table 1: *Approximate centre-of-mass energies and integrated luminosities delivered per experiment. In 1990 and 1991, a total of about 7 pb^{-1} was taken at off-peak energies, and 20 pb^{-1} per year in 1993 and in 1995. The total luminosity used by the experiments in the analyses was smaller by 10-15 % due to data taking inefficiencies.*

The data collected in 1989 constitute only a very small subset of the total statistics and are of lower quality, and therefore these are not used. In the years 1990 and 1991 "energy scans" were performed at seven different centre-of-mass energies around the peak of the Z resonance, placed about one GeV apart. In 1992 and 1994 there were high-statistics runs only at the peak energy. In 1993 and 1995 data taking took place at three energy points, about 1.8 GeV below and above the peak and at the peak. In particular the off-peak energies were carefully calibrated employing the technique of resonant depolarisation of the transversely polarised beams [11, 12, 13, 14].

The accumulated event statistics amounts to about 17 million Z decays recorded by the four experiments. A detailed break-down is given in Table 2.

year	A	D	L	O	all	year	A	D	L	O	all
			$q\overline{q}$						$\ell^+\ell^-$		
'90/91	433	357	416	454	1660	'90/91	53	36	39	58	186
'92	633	697	678	733	2741	'92	77	70	59	88	294
'93	630	682	646	642	2600	'93	78	75	64	79	296
'94	1640	1310	1359	1585	5894	'94	202	137	127	191	657
'95	735	659	526	652	2572	'95	90	66	54	81	291
total	4071	3705	3625	4066	15467	total	502	384	343	497	1724

Table 2: *The event statistics, in units of* 10^3*, used for the analysis of the* Z *line shape and lepton forward-backward asymmetries by the experiments* ALEPH *(A),* DELPHI *(D),* L3 *(L) and* OPAL *(O).*

As an example, the measurements of the hadronic cross-section at the three principal energy points are shown in Fig. 2. Because the hadron statistics are almost ten times larger than the lepton statistics, these measurements dominate the determination of the mass and the width of the Z. Detailed descriptions of the individual experimental analyses can be found in [1, 2, 3, 4]. They all rely on excellent separation of the final states, $q\overline{q}$, e^+e^-, $\mu^+\mu^-$ and $\tau^+\tau^-$, accompanied by high selection efficiencies. The total cross-section is determined from the number of selected events in a final state, N^f, the number of background events, $N_{\rm bg}$, the selection efficiency, ϵ, and the integrated luminosity, $\mathcal{L}$, $\sigma_{tot} = (N^f - N_{\rm bg})/(\epsilon\mathcal{L})$.

The luminosity of the beams is determined by normalisation to the process of small-angle Bhabha scattering, which is dominated by photon exchange in the t-channel. Thus, the integrated luminosity is given by the number of observed small-angle Bhabha events and the calculated cross-section for this process within a given angular acceptance. This requires the detection of back-to-back electrons and positrons close to the beam direction. Their positions and energies are precisely measured by forward calorimeters placed at small angles with respect to the beam line (typically 30 mrad$< \theta <$50 mrad). The main experimental systematic error arises from the definition of the geometrical acceptance for this process. Since the angular distribution is steeply falling with increasing scattering angle ($\propto \theta^{-3}$), the precise definition of the inner radius of the acceptance region is most critical.

The forward-backward asymmetry is defined by the numbers of events where the final state lepton is going forward or backward with respect to the direction of the incoming electron, N_f and N_b, respectively: $A_{\rm fb} = (N_f - N_b)/(N_f + N_b)$. In practice, $A_{\rm fb}$ is determined from a fit to the differential cross-section of the form $d\sigma/d\cos\theta \propto 1 + \cos^2\theta + 8/3 A_{\rm fb}\cos\theta$, where θ is the angle between of the final state fermion and the direction of the incoming electron. This procedure makes better use of the available information and hence leads to slightly smaller statistical errors. The electron final state is different due to t-channel

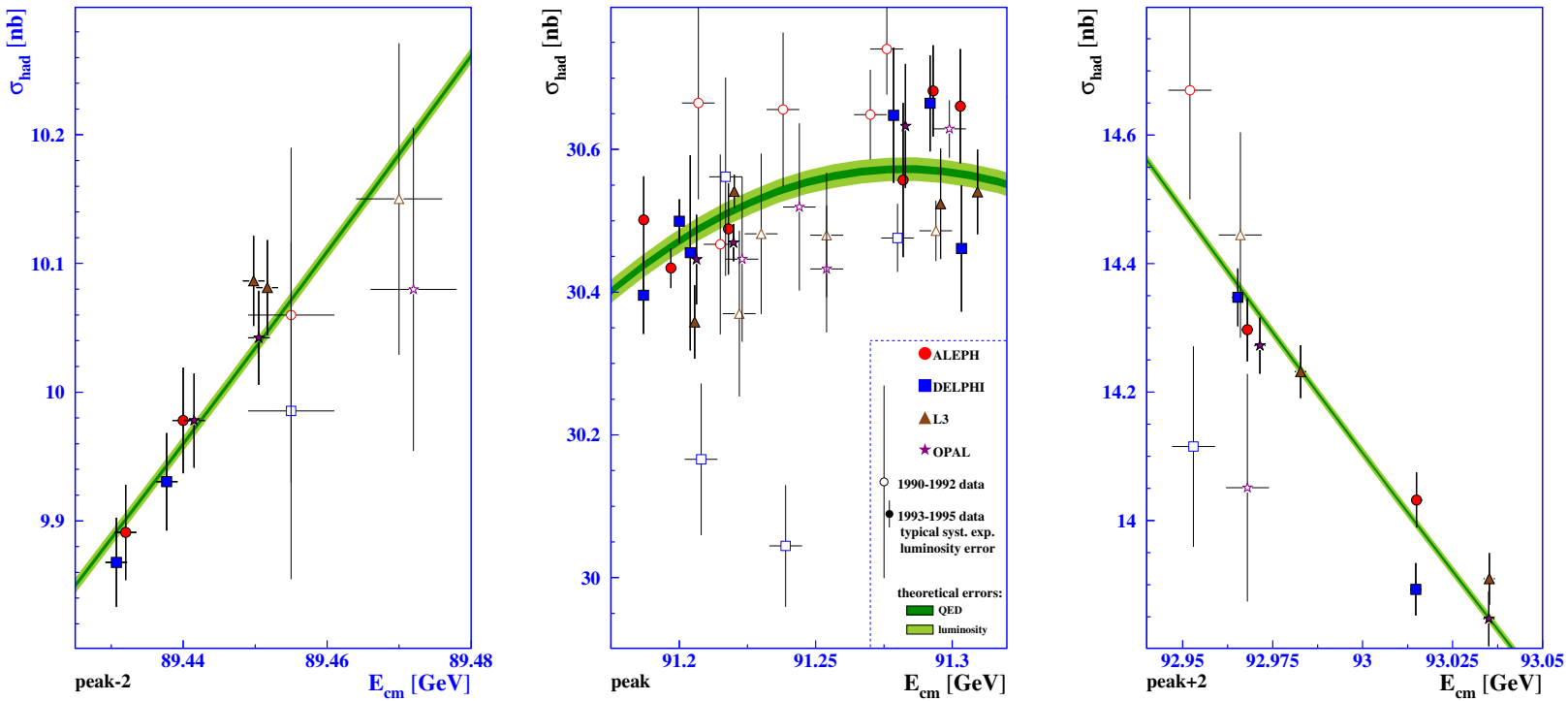

Figure 2: *Measurements by the four experiments of the hadronic cross-sections around the three principal energies. The vertical error bars show the statistical errors only. The open symbols represent the early measurements with typically much larger systematic errors than the later ones, shown as full symbols. Typical experimental systematic errors on the determination of the luminosity are also indicated; these are almost fully correlated within each experiment, but uncorrelated among the experiments. The horizontal error bars show the uncertainties in* LEP *centre-of-mass energy, where the errors for the period 1993–1995 are smaller than the symbol size in some cases. The bands represent the result of the model-independent fit to all data, including the two most important common theoretical errors from the unfolding of photon radiation and from the calculations of the small-angle Bhabha cross-section.*

diagrams, which is discussed in more detail in Sec. 5.2. The forward-backward asymmetries do not require any normalisation, but rely on precise measurements of the production angles of the final state fermions. This is difficult to achieve for quarks and, in addition, a full separation of all quark flavours is not possible. Therefore measurements of the forward-backward asymmetries in $q\overline{q}$ final states are not considered here.

In general, the systematic errors arising from the selection procedures are small and so the accumulated statistics can be fully exploited. Furthermore, the purely experimental errors arising from the limited understanding of detector acceptances are uncorrelated among the experiments. Errors arising from limitations in theoretical precision, such as the calculation of the small-angle Bhabha cross-section, the t-channel contribution in the e^+e^- final state or pure QED corrections to the cross-section, are common to all experiments. They are discussed in detail in section 5.

An overview of the experimental systematic errors is given in Table 3. The systematic error on the luminosity is common to all cross-section measurements, but does not affect the measurements of $A_{\rm fb}$.

	ALEPH			DELPHI		
	'93	'94	'95	'93	'94	'95
$\mathcal{L}^{\rm exp.}$	0.067%	0.073%	0.080%	0.24%	0.09%	0.09%
$\sigma_{\rm had}$	0.069%	0.072%	0.073%	0.10%	0.11%	0.10%
$\sigma_{\rm e}$	0.18%	0.16%	0.18%	0.46%	0.52%	0.52%
σ_{μ}	0.11%	0.09%	0.11%	0.28%	0.26%	0.28%
σ_{τ}	0.26%	0.18%	0.25%	0.60%	0.60%	0.60%
$A_{\rm fb}^{\rm e}$	0.0012	0.0012	0.0012	0.0026	0.0021	0.0020
$A_{\rm fb}^{\mu}$	0.0005	0.0005	0.0005	0.0009	0.0005	0.0010
$A_{\rm fb}^{\tau}$	0.0009	0.0007	0.0009	0.0020	0.0020	0.0020

	L3			OPAL		
	'93	'94	'95	'93	'94	'95
$\mathcal{L}^{\rm exp.}$	0.086%	0.064%	0.068%	0.033%	0.033%	0.034%
$\sigma_{\rm had}$	0.042%	0.041%	0.042%	0.073%	0.073%	0.085%
$\sigma_{\rm e}$	0.24%	0.17%	0.28%	0.17%	0.14%	0.16%
σ_{μ}	0.32%	0.31%	0.40%	0.16%	0.10%	0.12%
σ_{τ}	0.68%	0.65%	0.76%	0.49%	0.42%	0.48%
$A_{\rm fb}^{\rm e}$	0.0025	0.0025	0.0025	0.001	0.001	0.001
$A_{\rm fb}^{\mu}$	0.0008	0.0008	0.0015	0.0007	0.0004	0.0009
$A_{\rm fb}^{\tau}$	0.0032	0.0032	0.0032	0.0012	0.0012	0.0012

Table 3: *Experimental systematic errors for the analysis of the* Z *line shape and lepton forward-backward asymmetries at the* Z *peak. Except for the t-channel error none of the common errors discussed in Sec. 5 are included.*

2.2 Energy calibration

Precise knowledge of the centre-of-mass energy is essential for the determination of the mass and width of the Z resonance. The key features of the energy calibration procedure were the technique of resonant depolarisation and the careful monitoring of all relevant machine parameters [14]. The latter is important because beam energy calibrations with resonant depolarisation were possible only outside normal data taking, usually at the end of data taking in a particular fill of the accelerator, with fills typically lasting approximately 10 h. About 40% of the recorded off-peak luminosity was calibrated in this way in the 1993 scan and about 70% in the 1995 scan. For each experiment a value of the beam energy was provided every 15 minutes. These values were evaluated from the time evolutions of the relevant machine parameters. This required a model which took into account the fields in the LEP dipoles and in the corrector magnets, beam orbit positions, collision offsets at the interaction points and parameters of the radio-frequency system. In addition, also environmental effects from leakage currents produced by trains in the Geneva area and the gravitational forces of the Moon and the Sun leading to small deformations of the accelerator geometry had to be considered. Errors on the centre-of-mass energy are largely dominated by the uncertainties in this model. The energy errors vary slightly among the interaction points, largely due to different configurations of the radio frequency cavities. The energy errors for different experiments and periods of data taking have large common parts, and therefore the use of a full correlation matrix is necessary. Assuming that all experiments contribute with the same weight allows all the LEP energy errors to be conveniently summarised in a single error matrix, common to all interaction points, as given in Table 4.

The energy of individual beam particles is usually not at the mean value considered above, but oscillates around the mean energy. Therefore observables are not measured at a sharp energy, E^0_{cm}, but instead their values are averaged over a range in energies $E^0_{cm} \pm \delta E_{cm}$. With the assumption of a Gaussian shape of the energy distribution, the total cross-sections receive a correction proportional to $\delta {E_{cm}}^2$, which depends in leading order on the second derivative of $\sigma(E_{cm})$ w.r.t. E_{cm}. At LEP I, typical values of the beam energy spread are around 50 MeV. The effects of the correction lead to an increase of the cross-section at the peak of the Z resonance by 0.16% and a decrease of the width by about 5 MeV. The uncertainties on the energy spread, around ± 1 MeV in 1993–1995, constitute a negligible source of error common to all experiments.

In addition to the natural energy spread, changes in the mean beam energy due to changes of beam parameters have a similar effect. Periods of data taking with a very similar centre-of-mass energy were combined into a single energy point in the experimental analyses by performing a luminosity-weighted average. The additional energy spread resulting from this was only around 10 MeV, which adds in quadrature to the natural beam energy spread of the accelerator.

	'93 p-2	'93 p	'93 p+2	'94 p	'95 p-2	'95 p	'95 p+2
'93 p-2	3.42						
'93 p	2.76	6.69					
'93 p+2	2.59	2.64	2.95				
'94 p	2.25	2.38	2.16	3.62			
'95 p-2	1.29	1.14	1.23	1.23	1.78		
'95 p	1.19	1.20	1.25	1.30	1.24	5.39	
'95 p+2	1.20	1.15	1.33	1.24	1.22	1.34	1.68

Table 4: *Signed square root of covariance matrix elements, ($\mathcal{V}^E$), in* MeV*, from the determination of the centre-of-mass energies for the scan points in 1993–1995 [14]. Elements above the diagonal are left blank for simplicity. The errors for the earlier years may be found in Ref. [11, 12].*

3 Parametrisation of the differential cross-section

The differential cross-section for fermion pair production around the Z resonance consists of three s-channel contributions; from Z exchange, photon exchange and from the interference between photon and Z diagrams; $\sigma(s) = \sigma^{\mathrm{z}} + \sigma^{\gamma} + \sigma^{\mathrm{int}}$. This can be cast into a Born-type structure with complex-valued, s-dependent form factors describing the couplings of the Z and the photon to fermions. In the Z-pole approximation, valid for $s \simeq m_{\mathrm{Z}}^2$, these are taken to be constants. Neglecting initial and final state photon radiation, final state gluon radiation and fermion masses, the electroweak kernel cross-section can thus be written as

$$
\begin{aligned}
&\frac{2s}{\pi}\frac{1}{N_c^{\mathrm{f}}}\frac{d\sigma_{\mathrm{ew}}}{d\cos\theta}(\mathrm{e^+e^-} \to \mathrm{f\bar{f}}) \;=\\
&\underbrace{\left|\alpha(m_{\mathrm{Z}})Q^{\mathrm{f}}\right|^2 (1+\cos^2\theta)}_{\sigma^{\gamma}}\\
&\underbrace{-8\,\Re\left\{\alpha^*(m_{\mathrm{Z}})Q^{\mathrm{f}}\chi(s)\left[\mathcal{G}_V^{\mathrm{e}}\mathcal{G}_V^{\mathrm{f}}(1+\cos^2\theta)+2\mathcal{G}_A^{\mathrm{e}}\mathcal{G}_A^{\mathrm{f}}\cos\theta\right]\right\}}_{\sigma^{\mathrm{int}}}\\
&\underbrace{\begin{aligned}+16\,|\chi(s)|^2\Big[&(|\mathcal{G}_V^{\mathrm{e}}|^2+|\mathcal{G}_A^{\mathrm{e}}|^2)(|\mathcal{G}_V^{\mathrm{f}}|^2+|\mathcal{G}_A^{\mathrm{f}}|^2)(1+\cos^2\theta)\\ &+8\,\Re\left\{\mathcal{G}_V^{\mathrm{e}}\mathcal{G}_A^{\mathrm{e}\,*}\right\}\Re\left\{\mathcal{G}_V^{\mathrm{f}}\mathcal{G}_A^{\mathrm{f}\,*}\right\}\cos\theta\Big]\end{aligned}}_{\sigma^{\mathrm{z}}}
\end{aligned}
$$

with

$$\chi(s) = \frac{G_{\mathrm{F}} m_{\mathrm{Z}}^2}{8\pi\sqrt{2}}\,\frac{s}{s - m_{\mathrm{Z}}^2 + is\Gamma_{\mathrm{Z}}/m_{\mathrm{Z}}}\;.$$

Here $\alpha(m_{\mathrm{Z}})$ is the electromagnetic coupling constant at the scale of the Z mass, G_{F} is the Fermi constant, Q_{f} is the charge of the final state fermion, and the colour factor N_c^{f} is one for leptons (f=e, μ, τ) and three for quarks (f=u, d, s, c, b). $\mathcal{G}_V^{\mathrm{f}}$ and $\mathcal{G}_A^{\mathrm{f}}$ are the effective

vector and axial vector couplings of fermions to the Z. $\chi(s)$ is the propagator term with a Breit-Wigner denominator with an s-dependent width.

In Bhabha final states, $e^+e^- \to e^+e^-$, also the t-channel diagrams contribute to the cross-sections, with a very dominant contribution at large $\cos\theta$, *i.e.* in the forward direction. This contribution, and also its interference with the s-channel, add to the pure s-channel cross section for $e^+e^- \to e^+e^-$. (See Sec. 5.2 for details.)

The $1+\cos^2\theta$ terms in the above formula contribute to the total cross-section, whereas the terms multiplying $\cos\theta$ contribute only to the forward-backward asymmetries for an experimental acceptance symmetric in $\cos\theta$. The total cross-section is completely dominated by Z exchange. The $\gamma - \mathrm{Z}$ interference determines the energy dependence of the forward-backward asymmetries and dominates at off-peak energies, but the leading contribution from the real parts of the couplings vanishes at $\sqrt{(}s) = m_\mathrm{Z}$.

The inclusion of higher-order electroweak corrections is absorbed in $\mathcal{G}_A$ and $\mathcal{G}_V$ with small imaginary parts arising from electroweak form factors. The experimental measurements do not allow a simultaneous extraction of the real and imaginary parts, and therefore the effective couplings to be determined are defined as $g_A = \mathrm{Re}(\mathcal{G}_A)$ and $g_V = \mathrm{Re}(\mathcal{G}_V)$. The imaginary parts of $\mathcal{G}_A$ and $\mathcal{G}_V$ are explicitly accounted for in the fitting codes by setting them to their SM expectations. The effects of box diagrams are also taken into account at this level.

It is worth noting that the definitions of the mass and width with an s-dependent width term in the Breit-Wigner denominator are suggested by phase-space and the structure of the electroweak radiative corrections within the SM. They are different from other commonly used definitions, *e. g.* the real part of the pole position in the energy-squared plane, where the propagator term takes the form $\chi(s) \propto s/(s - \overline{\mathrm{m}}_\mathrm{Z}{}^2 + i\,\overline{\mathrm{m}}_\mathrm{Z}\overline{\Gamma}_\mathrm{Z})$; $\overline{\mathrm{m}}_\mathrm{Z}$ and $\overline{\Gamma}_\mathrm{Z}$ are different from m_Z and Γ_Z by a multiplicative factor $1/\sqrt{1+\Gamma_\mathrm{Z}^2/m_\mathrm{Z}^2}$.

Photon radiation from the initial and final states, and their interference, is conveniently treated by convoluting the electroweak kernel cross-section, $\sigma_{ew}(s)$, with a QED radiator, H_{QED},

$$\sigma(s) = \int dz\, H_{QED}(z,s)\, \sigma_{ew}(zs)\,.$$

At the peak the QED de-convoluted cross-section is 36 % larger than the measured one, and the peak position is shifted downwards by about 100 MeV. The estimated precision of this important correction is discussed in Sec. 5.4.1.

The partial Z decay widths are defined inclusively, *i.e.* they contain QED and QCD final state corrections and the contribution from the imaginary parts of the effective couplings,

$$\Gamma_\mathrm{ff} = N_c^\mathrm{f}\,\frac{G_\mathrm{F}\,m_\mathrm{Z}^3}{6\sqrt{2}\pi}\,\left(|\mathcal{G}_A^\mathrm{f}|^2 R_A^\mathrm{f} \,+\, |\mathcal{G}_V^\mathrm{f}|^2 R_V^\mathrm{f}\right) \,+\, \Delta_{ew/QCD}\,.$$

The radiator factors R_V^f and R_A^f take into account final state QED and QCD corretions as well as non-zero fermion masses; $\Delta_{ew/QCD}$ accounts for non-factorizable electroweak/QCD corrections. The inclusion of the imaginary parts of the couplings in the definition of the leptonic width, $\Gamma_{\ell\ell}$, leads to changes of 0.15 per-mille corresponding to only 15 % of the LEP-combined experimental error on $\Gamma_{\ell\ell}$.

The total cross-section arising from the $\cos\theta$-symmetric Z production term can also be written in terms of the partial decay widths into the initial and final states, Γ_{ee} and Γ_{ff},

$$\sigma_{\mathrm{f\bar{f}}}^{\mathrm{Z}} = \sigma_{\mathrm{f\bar{f}}}^{\mathrm{peak}} \frac{s\,\Gamma_{\mathrm{Z}}^2}{(s-m_{\mathrm{Z}})^2 + s^2\Gamma_{\mathrm{Z}}^2/m_{\mathrm{Z}}^2},$$

$$\text{with } \sigma_{\mathrm{f\bar{f}}}^{\mathrm{peak}} = \frac{1}{1+\delta_{\mathrm{QED}}}\sigma_{\mathrm{f\bar{f}}}^{0} \text{ and } \sigma_{\mathrm{f\bar{f}}}^{0} = \frac{12\,\pi}{m_{\mathrm{Z}}^2}\,\frac{\Gamma_{\mathrm{ee}}\Gamma_{\mathrm{ff}}}{\Gamma_{\mathrm{Z}}}\,.$$

The term $1/(1+\delta_{\mathrm{QED}})$ takes out the final state QED correction included in the definition of Γ_{ee}.

No distinction of the flavours of produced quarks is made, and therefore the overall hadronic cross-section is measured, and is parameterised in terms of the hadronic width given by the sum over all quark final states,

$$\Gamma_{\mathrm{had}} = \sum_{\mathrm{q},\,\mathrm{q}\neq\mathrm{t}} \Gamma_{\mathrm{q\bar{q}}}\,.$$

Z decays to neutrinos are invisible in the detecors and give rise to the "invisible width", $\Gamma_{\mathrm{inv}} = N_\nu\Gamma_{\nu\nu}$, where N_ν is the number of light neutrino species. Γ_{inv} can be determined from the measurements of the decay widths to all visible final states and the total width, which is given by the sum over all partial widths,

$$\Gamma_{\mathrm{Z}} = \Gamma_{\mathrm{ee}} + \Gamma_{\mu\mu} + \Gamma_{\tau\tau} + \Gamma_{\mathrm{had}} + \Gamma_{\mathrm{inv}}\,.$$

Because the measured cross-sections depend on products of the partial widths and also on the total width, the widths constitute a highly correlated parameter set. In order to reduce correlations among the fit parameters an experimentally-motivated set of six parameters is used to describe the total hadronic and leptonic cross-sections around the Z peak. These are

- the mass of the Z, m_{Z}, and the total width, Γ_{Z};
- the "hadronic pole cross-section",

$$\sigma_{\mathrm{h}}^{o} \equiv \frac{12\pi}{m_{\mathrm{Z}}^2}\frac{\Gamma_{\mathrm{ee}}\Gamma_{\mathrm{had}}}{\Gamma_{\mathrm{Z}}^2}\,;$$

- the ratios

$$R_{\mathrm{e}} \equiv \Gamma_{\mathrm{had}}/\Gamma_{\mathrm{ee}}\,,\ R_\mu \equiv \Gamma_{\mathrm{had}}/\Gamma_{\mu\mu} \text{ and } R_\tau \equiv \Gamma_{\mathrm{had}}/\Gamma_{\tau\tau}\,.$$

The leading contribution from $\gamma-\mathrm{Z}$ interference is proportional to the product of the vector couplings of the initial and final states and vanishes at $\sqrt{s} = m_{\mathrm{Z}}$, but becomes noticeable at off-peak energies and therefore affects the Z mass. Because a determination of all quark couplings is not possible, the $\gamma-\mathrm{Z}$ interference term in the hadronic final state is fixed to its SM value. The implications of this are discussed in Sec. 6.4.

Three additional parameters are needed to describe the leptonic forward-backward asymmetries. These are the "pole asymmetries", $A_{FB}^{0,e}$, $A_{FB}^{0,\mu}$ and $A_{FB}^{0,\tau}$ for the processes $e^+e^- \to e^+e^-$, $e^+e^- \to \mu^+\mu^-$ and $e^+e^- \to \tau^+\tau^-$. Contrary to the case of the partial widths, the pole asymmetries are defined purely in terms of the real parts of the effective Z couplings,

$$A_{FB}^{0,f} \equiv \frac{3}{4}\mathcal{A}_e\mathcal{A}_f \quad \text{with} \quad \mathcal{A}_f = \frac{2\, g_V^f / g_A^f}{1 + \left(g_V^f / g_A^f\right)^2}\,.$$

Due to the smallness of the leptonic forward-backward asymmetry at $\sqrt{s} = m_Z$, QED corrections are as large as $A_{FB}^{0,\ell}$ itself. The leading contribution of the $\gamma - Z$ interference is proportional to the product of the axial vector couplings of the initial and final state and can be fixed by performing simultaneous fits to the measured forward-backward asymmetries and cross-sections, requiring SM input only for the imaginary parts of the couplings.

Differences between the pseudo-observables and the QED de-convoluted observables at $\sqrt{s} = m_Z$, arising from the interference between photon and Z diagrams and from the interplay between the real and imaginary parts of the photon and Z couplings, are small in the SM. $\sigma_{f\bar{f}}^{peak}$, given in terms of the partial decay widths, agrees to better than 0.5 per-mille for both hadrons and leptons with the QED de-convoluted cross-sections without the photon exchange contribution at $\sqrt{s} = m_Z$. This is only a fraction of the LEP-combined experimental error. The difference between $A_{FB}^{0,\ell}$ and the QED de-convoluted forward-backward asymmetry at the peak amounts to 0.0013, which is slightly larger than the LEP-combined error on $A_{FB}^{0,\ell}$. It is therefore important to treat the imaginary parts correctly, but there is no sensitivity to electroweak corrections within the SM.

The pseudo-observables introduced above cannot be considered as truly model-independent, because imaginary parts of the couplings as well as the $\gamma - Z$ interference in the hadronic final state need to be fixed to their SM values. This leads to small "Standard Model remnants" in any attempted "model-independent" definition of the pseudo-observables. More details about the treatment of imaginary parts and SM remnants in the theory programs TOPAZ0 [15] and ZFITTER [16] are given in Ref. [17]. These computer codes make available the best up-to-date knowledge on QED and electroweak corrections within the minimal Standard Model and also provide a (quasi) model-independent approach based on the parametrisation of the cross-sections and forward-backward asymmetries above.

4 Experimental results

The experimental results presented here deviate slightly from those published by the experiments in order to facilitate the combination procedure. All fits are based on the versions 6.23 of ZFITTER and 4.4 of TOPAZ0. Each experiment used the combined energy error matrix described above (Tab.4). In the Bhabha final state, the treatment of the dependence of the s–t interference on the Z mass presented here is the same (see Sec.5.2 below), despite

some different choices in the publications of the individual results. The four dedicated sets of experimental results for the combination are summarised in Tab. 5.

5 Common errors

Important common errors among the results from all LEP experiments arise from several sources. These are the calibration of the beam energy, the theoretical error on the calculation of the small-angle Bhabha cross-section used as the normalisation reaction, the theoretical uncertainties in the t-channel and s–t interference contribution to the differential large-angle Bhabha cross-section, the theoretical uncertainties in the calculations of QED radiative effects and, finally, from small uncertainties in the parametrisation of the electroweak cross-section near the Z resonance in terms of the set of pseudo-observables the four collaborations agreed upon. These common errors are quantified in the sub-sections below and will be used in the combination.

Other sources of common errors may arise from the use of common Monte Carlo generators and detector simulation programs. However, each group uses its own tuning procedures and event selections which best suit their detector, and therefore the related errors are treated as uncorrelated among the experiments.

5.1 Common energy errors

For the purpose of combining the experimental results at the parameter level, the errors on the centre-of-mass energy of each individual cross-section or asymmetry measurement, as given in Table 4, need to be transformed into errors on the extracted pseudo-observables. The first step is to scale the energy errors by factors of $1 \pm \epsilon$, while maintaining the experimental errors fixed. Typical values of ϵ used are between 5 % and 20 %. Performing the standard fits with these scaled errors generates two pseudo-observable covariance matrices, $V_{\pm}$, from which the covariance matrix due to energy errors, V_E, can be separated from the other errors, $V_{\rm exp}$, using the relation $(V_{\pm}) = (1 \pm \epsilon)^2 (V_E) + (V_{\rm exp})$. The validity of this procedure was verified using a data set restricted to the hadronic cross-section measurements of the years 1993–1995, which were combined both at the cross-section level and at the parameter level [18].

Tab. 15 and 16 in the appendix show the errors on the pseudo-observables extracted from the individual experimental data sets. The estimated energy errors differ slightly depending on which experimental data set is used to derive them. Combinations may be attempted based on each of them, or on the average. The central values and errors of each of the averaged parameters agree to well within 5 % of the error on that average. It is therefore most appropriate to take the average of the error estimates over the experiments as the common energy errors, which are shown in Tab. 6.

$\chi^2/N_{\rm df}$ = 169/176		ALEPH								
$m_{\rm Z}$ [GeV]	91.1891 ± 0.0031	1.00	.038	-.091	.102	-.003	-.003	-.047	.072	.061
$\Gamma_{\rm Z}$ [GeV]	2.4959 ± 0.0043	.038	1.00	-.383	.004	.012	.004	.000	.002	.002
$\sigma^o_{\rm h}$ [nb]	41.558 ± 0.057	-.091	-.383	1.00	.134	.167	.152	-.003	.002	.002
$R_{\rm e}$	20.690 ± 0.075	.102	.004	.134	1.00	.083	.067	-.388	.019	.017
R_μ	20.801 ± 0.056	-.003	.012	.167	.083	1.00	.093	.000	.013	.000
R_τ	20.708 ± 0.062	-.003	.004	.152	.067	.093	1.00	.000	.000	.011
$A_{\rm FB}^{0,{\rm e}}$	0.0184 ± 0.0034	-.047	.000	-.003	-.388	.000	.000	1.00	-.008	-.007
$A_{\rm FB}^{0,\mu}$	0.0172 ± 0.0024	.072	.002	.002	.019	.013	.000	-.008	1.00	.016
$A_{\rm FB}^{0,\tau}$	0.0170 ± 0.0028	.061	.002	.002	.017	.000	.011	-.007	.016	1.00

$\chi^2/N_{\rm df}$ = 177/168		DELPHI								
$m_{\rm Z}$ [GeV]	91.1864 ± 0.0028	1.00	.047	-.070	.063	-.003	.001	.057	.064	.043
$\Gamma_{\rm Z}$ [GeV]	2.4876 ± 0.0041	.047	1.00	-.270	.000	-.007	-.001	.001	.006	.003
$\sigma^o_{\rm h}$ [nb]	41.578 ± 0.069	-.070	-.270	1.00	.120	.191	.113	-.006	-.002	-.002
$R_{\rm e}$	20.88 ± 0.12	.063	.000	.120	1.00	.054	.033	-.106	.025	.015
R_μ	20.650 ± 0.076	-.003	-.007	.191	.054	1.00	.051	.000	.008	.000
R_τ	20.84 ± 0.13	.001	-.001	.113	.033	.051	1.00	-.001	.000	.012
$A_{\rm FB}^{0,{\rm e}}$	0.0171 ± 0.0049	.057	.001	-.006	-.106	.000	-.001	1.00	-.016	-.015
$A_{\rm FB}^{0,\mu}$	0.0165 ± 0.0025	.064	.006	-.002	.025	.008	.000	-.016	1.00	.014
$A_{\rm FB}^{0,\tau}$	0.0241 ± 0.0037	.043	.003	-.002	.015	.000	.012	-.015	.014	1.00

$\chi^2/N_{\rm df}$ = 158/166		L3								
$m_{\rm Z}$ [GeV]	91.1897 ± 0.0030	1.00	.065	.009	.108	-.001	.002	-.045	.052	.034
$\Gamma_{\rm Z}$ [GeV]	2.5025 ± 0.0041	.065	1.00	-.343	-.007	.002	.005	.055	.004	.004
$\sigma^o_{\rm h}$ [nb]	41.535 ± 0.054	.009	-.343	1.00	.075	.077	.053	-.006	.005	.003
$R_{\rm e}$	20.815 ± 0.089	.108	-.007	.075	1.00	.030	.024	-.146	.017	.012
R_μ	20.861 ± 0.097	-.001	.002	.077	.030	1.00	.020	-.001	.005	.000
R_τ	20.79 ± 0.13	.002	.005	.053	.024	.020	1.00	-.003	.000	.007
$A_{\rm FB}^{0,{\rm e}}$	0.0107 ± 0.0058	-.045	.055	-.006	-.146	-.001	-.003	1.00	.011	-.008
$A_{\rm FB}^{0,\mu}$	0.0188 ± 0.0033	.052	.004	.005	.017	.005	.000	.011	1.00	.006
$A_{\rm FB}^{0,\tau}$	0.0260 ± 0.0047	.034	.004	.003	.012	.000	.007	-.008	.006	1.00

$\chi^2/N_{\rm df}$ = 155/194		OPAL								
$m_{\rm Z}$ [GeV]	91.1858 ± 0.0030	1.00	.049	.031	.108	.001	.001	-.053	.077	.059
$\Gamma_{\rm Z}$ [GeV]	2.4948 ± 0.0041	.049	1.00	-.352	.011	.020	.013	-.005	-.002	-.003
$\sigma^o_{\rm h}$ [nb]	41.501 ± 0.055	.031	-.352	1.00	.155	.222	.137	.011	.011	.003
$R_{\rm e}$	20.901 ± 0.084	.108	.011	.155	1.00	.093	.039	-.222	.031	.015
R_μ	20.811 ± 0.058	.001	.020	.222	.093	1.00	.051	-.001	.018	-.010
R_τ	20.832 ± 0.091	.001	.013	.137	.039	.051	1.00	.005	.004	.007
$A_{\rm FB}^{0,{\rm e}}$	0.0089 ± 0.0045	-.053	-.005	.011	-.222	-.001	.005	1.00	-.012	-.010
$A_{\rm FB}^{0,\mu}$	0.0159 ± 0.0023	.077	-.002	.011	.031	.018	.004	-.012	1.00	.013
$A_{\rm FB}^{0,\tau}$	0.0145 ± 0.0030	.059	-.003	.003	.015	-.010	.007	-.010	.013	1.00

Table 5: *Results on Z parameters obtained with ZFITTER vers. 6.23 and error correlation matrices by the four experiments.* **Opal numbers not yet approved for publication!**

	m_{Z}	Γ_{Z}	σ^{o}_{h}	R_{e}
m_{Z}	0.0017			
Γ_{Z}	−0.0006	0.0012		
σ^{o}_{h}	−0.0018	−0.0027	0.011	
R_{e}	0.0017	−0.0014	0.0073	0.013

	$A^{0,\mathrm{e}}_{\mathrm{FB}}$	$A^{0,\mu}_{\mathrm{FB}}$	$A^{0,\tau}_{\mathrm{FB}}$
$A^{0,\mathrm{e}}_{\mathrm{FB}}$	0.0004		
$A^{0,\mu}_{\mathrm{FB}}$	−0.0003	0.0003	
$A^{0,\tau}_{\mathrm{FB}}$	−0.0003	0.0003	0.0003

Table 6: *Common energy errors for nine-parameter fits. Values are given as the signed square root of the covariance matrix elements; elements above the diagonal have been omitted for simplicity. The anti-correlation between electron and muon or tau asymmetries arises from the different energy dependence of the electron asymmetry due to the t-channel contribution.*

5.2 Common t-channel errors

The t channel and s–t interference contributions are calculated in the Standard Model using the program ALIBABA [19]. The s–t interference contribution to the t-channel correction in Bhabha final states depends on the particular value of the Z mass. For the purpose of this combination, all experiments parametrise the t and s–t contributions as a function of m_{Z}. This allows the t, s–t correction to follow their own determination of m_{Z} in the fits, which results in a correlation between m_{Z} and R_{e} or $A^{0,\mathrm{e}}_{\mathrm{FB}}$. The change in correlation coefficients introduced by explicitly taking into account in the fits the m_{Z} dependence of the t-channel is about $+10\,\%$ for the correlation m_{Z}–R_{e} and $-10\,\%$ for m_{Z}–$A^{0,\mathrm{e}}_{\mathrm{FB}}$. These correlation coefficients properly take into account the changes in R_{e} and $A^{0,\mathrm{e}}_{\mathrm{FB}}$ when m_{Z} takes its average value in the combination of the four experiments.

The theoretical uncertainty on the t-channel correction is discussed in detail in Ref. [20]. The size of the uncertainty is typically 1.1 pb for the forward cross-section and 0.3 pb for the backward cross-section and depends slightly on the acceptance cuts [21]. All collaborations incorporate the theory uncertainty as an additional error on the electron pair cross-section and asymmetry. In order to evaluate the common error due to the t, $s-t$ theory error, each collaboration performed two fits, with and without the theory error, and the quadratic differences of the covariance matrix elements for R_{e} and $A^{0,\mathrm{e}}_{\mathrm{FB}}$ are taken as an estimate of the common error. The unknown error correlation between energy points below and above the peak are included in the error estimates by adding in quadrature the observed shifts in mean values of R_{e} and $A^{0,\mathrm{e}}_{\mathrm{FB}}$ when varying these correlations between -1 and $+1$. The t, $s-t$-channel errors estimated by individual experiments are summarised in Tab. 17 in the appendix. Since these are all very similar, the average shown in Tab. 7 is taken as the common error matrix.

5.3 Common luminosity errors

The four collaborations use similar techniques to measure the luminosity of their data samples by counting the number of small–angle Bhabha scattered electrons. The experimental details of the four measurements differ sufficiently that no correlation is believed to exist in the experimental component of the luminosity errors. All four collaborations, however,

	R_{e}	$A_{\mathrm{FB}}^{0,\mathrm{e}}$
R_{e}	0.024	
$A_{\mathrm{FB}}^{0,\mathrm{e}}$	−0.0054	0.0014

Table 7: *Common t, $s-t$-channel errors, given as the signed square root of the covariance matrix elements.*

use BHLUMI 4.04 [22], the best available theoretical model of small–angle Bhabha scattering, to calculate the acceptance of their luminosity counters for the bulk of their data. Therefore significant correlations exist in the errors assigned to the scale of the measured cross-sections due to the uncertainty in this common theoretical calculation.

This uncertainty is estimated to be 0.061 % [23] without applying a correction for the production of light fermion pairs, which are not calculated in BHLUMI, and enter as a contribution to the estimated error. A recent calculation of the contribution of light pairs [24] has allowed OPAL to explicitly correct for light pairs and reduce its theoretical luminosity uncertainty to 0.054 %. This 0.054 % error is taken to be correlated with the errors of the other three experiments, who between themselves share a mutual correlated error of 0.061 %

These errors almost exclusively affect the hadronic pole cross-section, and contribute about half its total error after combination. The common luminosity error also introduces a small contribution to the covariance matrix element between Γ_{Z} and σ_{h}^{o}. This was neglected in the common error tables given above, as it had no noticeable effect on the combined result.

5.4 Common theory errors

An additional class of common theoretical errors arises from the approximations and special choices made in the fitting codes. These comprise contributions from QED radiative corrections, including initial-state pair radiation, and the parametrisation of the differential cross-section around the Z resonance in terms of pseudo-observables defined precisely at the peak and for pure Z exchange only. In order to estimate the uncertainties from the parametrisation of the electroweak cross-sections near the Z resonance the two most advanced calculational tools, ZFITTER [16], and TOPAZ0 [15] were compared. In addition, there are "parametric uncertainties" arising from parameters of the SM that are needed to fix the SM remnants.

5.4.1 QED errors

The effects of initial state radiation (ISR) and the radiation of fermion pairs (ISPP) lead to large corrections in the vicinity of the Z resonance and therefore play a central role in the extraction of the pseudo-observables from the measured cross-sections and asymmetries. Such large radiative effects have to be seen in contrast to the experimental precision, which

is below the per-mille level in the case of the hadronic cross-section.

The most up-to-date evaluations of photonic corrections include the leading contributions up to $\mathcal{O}(\alpha^3)$. Two different schemes are available to estimate the remaining uncertainties:

1. KF: O(... α^2L^2,α^2L,α^2L^0) calculations [25] including the exponentiation scheme of Kuraev-Fadin [26] with O(α^3L^3) [27]. [3)]

2. YFS: the 2$^{\rm nd}$ order inclusive exponentiation scheme of Ref. [28, 29], based on the YFS approach [30]. Third order terms are known and have only a small effect [31].

Differences between these schemes implemented in ZFITTER, TOPAZ0 and MIZA [32], and uncertainties due to missing higher order corrections [31], amount to at most ± 0.1 MeV on $m_{\rm Z}$ and $\Gamma_{\rm Z}$, and $\pm 0.01\,\%$ on $\sigma^o_{\rm h}$.

The influence of the interference between initial and final state radiation on the extracted parameters has also been studied recently [33], and uncertainties on $m_{\rm Z}$ of at most ± 0.1MeV from this source are expected for the experimental results given with only a small cut on s', the effective squared centre-of-mass energy after photon radiation from the initial state. The uncertainties due to the extrapolation of the leptonic s-channel cross-sections to full angular acceptance and from large to small s' are different among the experiments and are believed to be largely uncorrelated.

QED related uncertainties are dominated by the radiation of fermion pairs from the initial state. Starting from the full second order pair radiator [25, 34], a simultaneous exponentiation scheme for radiated photons and pairs was proposed in Ref. [35]. A third-order pair radiator was calculated recently [36] and compared with the other existing schemes, which are all available in the latest version of ZFITTER. Independent implementations of some schemes exist in TOPAZ0 and in MIZA. The largest uncertainty arises from the contribution of hadronic pairs. The maximum differences are 0.3 MeV on $m_{\rm Z}$, 0.2 MeV on $\Gamma_{\rm Z}$ and 0.015 % on $\sigma^o_{\rm h}$.

In summary, comparing the different options for photonic and fermion pair radiation leads to error estimates of ± 0.3 MeV on $m_{\rm Z}$ and ± 0.2 MeV on $\Gamma_{\rm Z}$. The observed differences in $\sigma^o_{\rm h}$ are slightly smaller than the error estimate of $\pm 0.02\,\%$ in Ref. [31], which is therefore taken as the error in this case.

5.4.2 Parametrisation of line shape and asymmetries

In a recent very detailed comparison of TOPAZ0 and ZFITTER [17], cross-sections from Standard Model calculations and from the model-independent parametrisation were considered. Uncertainties on the pseudo-observables arise from the parametrisation of the electroweak cross-sections near the Z resonance. In order to determine these, each of the two codes could be used in an iterative fit procedure. For practical reasons, however, a different approach was taken: cross-sections and forward-backward asymmetries were

[3)] Third-order terms for the KF scheme had also been calculated earlier [28].

Δm_{Z} [GeV]	$\Delta\Gamma_{\mathrm{Z}}$ [GeV]	$\Delta\sigma^{o}_{\mathrm{h}}$ [nb]	ΔR_{ℓ}	$\Delta A^{0,\ell}_{\mathrm{FB}}$
0.0001	0.0001	0.001	0.004	0.0001

Table 8: *Differences in fit results obtained with TOPAZ0 and ZFITTER, taken as common systematic errors.*

calculated with TOPAZ0 and then fitted with ZFITTER. Errors were assigned to the calculated cross-sections and forward-backward asymmetries which reflected the integrated luminosity taken at each energy, thus ensuring that each energy point entered with the appropriate weight.

The dominant difference between the two codes results from the implementation of the cross-section parametrisation in terms of pseudo-observables, where the energy points away from the peak of the resonance are of particular importance. The size of the differences depends on the particular point in parameter space at which they are evaluated, because the measured parameters do not respect the exact Standard Model relations due to measurement errors. Variations of the electroweak calculations may affect the fit results through the SM remnants, but were found to have a negligible effect.

The differences between TOPAZ0 and ZFITTER were evaluated around the set of pseudo-observables representing the average of the four experiments, where the cross-sections and asymmetries were calculated for full acceptance with only a cut in s', with $s' > 0.01\,s$. The result is shown in Tab. 8. The only important systematic error of this kind is the one on R_{ℓ}, which amounts to 15 % of the combined error.

Putting all sources together, overall theoretical errors as listed in Tab. 9 are obtained, and these are used in the combination.

	m_{Z}	Γ_{Z}	σ^{o}_{h}	R_{e}	R_{μ}	R_{τ}	$A^{0,\mathrm{e}}_{\mathrm{FB}}$	$A^{0,\mu}_{\mathrm{FB}}$	$A^{0,\tau}_{\mathrm{FB}}$
m_{Z}[GeV]	0.0003								
Γ_{Z}[GeV]		0.0002							
σ^{o}_{h}[nb]			0.008						
R_{e}				0.004					
R_{μ}				0.004	0.004				
R_{τ}				0.004	0.004	0.004			
$A^{0,\mathrm{e}}_{\mathrm{FB}}$							0.0001		
$A^{0,\mu}_{\mathrm{FB}}$							0.0001	0.0001	
$A^{0,\tau}_{\mathrm{FB}}$							0.0001	0.0001	0.0001

Table 9: *Theoretical errors from fit programs, i.e. photon and fermion-pair radiation and model-independent parametrisation, given as the signed square root of the covariance matrix elements.*

5.4.3 Parametric uncertainties

The LEP experiments agreed to use a standard set of SM parameters to fix the Standard Model remnants in the fitting codes. These are $m_{\rm Z} = 91.187\,\GeV$, $M_{\rm t} = 175\,\GeV$, $M_{\rm H} = 150\,\GeV$, $\alpha_s(m_{\rm Z}) = 0.119$ and $\alpha^{(5)}(m_{\rm Z}) = 1/128.878$ [4]. Varying these parameters within their present experimental errors, or between 100 GeV and 1000 GeV in case of the Higgs boson mass, leads to observable effects only on the Z mass, which is affected through the γ–Z interference term. The dominant dependence is on $M_{\rm H}$, followed by $\alpha^{(5)}$. The change in $m_{\rm Z}$ due to $M_{\rm H}$ amounts to $+0.23$ MeV per unit change in $\log_{10}(M_{\rm H}/\GeV)$, and the change is ∓ 0.05 MeV for a change in $1/\alpha^{(5)}(m_{\rm Z})$ by its error of ± 0.090, which is small compared to the combined error on $m_{\rm Z}$ of ± 2.1 MeV.

The effect of a completely model-independent treatment of the γ–*Zzero* interference and its influence on the extracted Z parameters is discussed in Sec. 6.4 below.

6 Combination of results

The combination of results on the Z parameters is based on the nine parameters $m_{\rm Z}$, $\Gamma_{\rm Z}$, $\sigma^o_{\rm h}$, $R_{\rm e}$, R_μ, R_τ, $A^{0,\,e}_{\rm FB}$, $A^{0,\,\mu}_{\rm FB}$ and $A^{0,\,\tau}_{\rm FB}$ and the common errors given in the previous chapter.

For this purpose it is necessary to construct the full $(4\times 9)\times(4\times 9)$ covariance matrix of the errors. The four diagonal 9×9 matrices consist of the four error matrices specified by each experiment (Tab. 5). The 9×9 common error matrices build the off-diagonal elements. Some theoretical uncertainties must also be added to the diagonal matrices, since they are not contained in the individual experimental matrices.

A symbolic representation of this matrix is shown in Table 10 . Each table element represents a 9×9 matrix; $(\mathcal{C}_{exp})$ for exp = A, D, L and O are the covariance matrices of the experiments (see Tab. 5), and $(\mathcal{C}_c) = (\mathcal{C}_E) + (\mathcal{C}_\mathcal{L}) + (\mathcal{C}_t) + (\mathcal{C}_{\rm QED,th})$ is the matrix of common errors. (C_E) (Tab. 6) is the error matrix due to LEP energy uncertainties, $(C_\mathcal{L})$ (Sec. 5.3) arises from the theoretical error on the small-angle Bhabha cross-section calculations, C_t (Tab. 7) contains the errors from the t-channel treatment in the $\rm e^+e^-$ final state, and $(\mathcal{C}_{\rm QED,th})$ contains the errors from initial state photon and fermion pair radiation and from the model-independent parametrisation (Tab. 9). Since the latter errors were not included in the experimental error matrices, they were also added to the block matrices in the diagonal of Table 10 .

The combined parameter set and its covariance matrix are obtained from a χ^2 minimisation, with

$$\chi^2 = (\mathbf{X}-\mathbf{X_m})^T(\mathcal{C})^{-1}(\mathbf{X}-\mathbf{X_m}); \qquad (1)$$

$(\mathbf{X}-\mathbf{X_m})$ is the vector of residuals of the combined parameter set to the individual results.

Some checks of the combination procedure outlined above are described in the following subsections, and the combined results are given in the tables of Sec. 6.6.

[4] $\alpha^{(5)}(m_{\rm Z})$ is the electromagnetic coupling constant at the scale of the Z mass for five quark flavours; the value and error given correspond to a value of the correction due to hadronic vacuum polarisation of $\Delta\alpha^{(5)}_{\rm had} = 0.02804 \pm 0.00065$.

$(\mathcal{C})$	ALEPH	DELPHI	L3	OPAL
A	$(\mathcal{C}_A) + (\mathcal{C}_{\rm QED,th})$			
D	(C_c)	$(\mathcal{C}_D) + (\mathcal{C}_{\rm QED,th})$		
L	(C_c)	(C_c)	$(\mathcal{C}_L) + (\mathcal{C}_{\rm QED,th})$	
O	(C_c)	(C_c)	(C_c)	$(\mathcal{C}_O) + (\mathcal{C}_{\rm QED,th})$

Table 10: *Symbolic representation of the covariance matrix,* $(\mathcal{C})$*, used to combine the line shape and asymmetry results of the four experiments. Elements above the diagonal are the same as those above, but are left blank for simplicity. The components of the matrix are explained in the text.*

6.1 Multiple-$m_{\rm Z}$ fits

In 1993 and 1995, the two years when LEP performed precision scans to measure the Z line shape, the experimental errors are very comparable, but the LEP energy was appreciably better understood in 1995 than in 1993. In determining the optimum value of $m_{\rm Z}$, therefore, the four experiments combined should give more weight to the 1995 data than they each do in their independent determinations. To quantify this issue the measurements of each experiment were fitted to determine an independent value of $m_{\rm Z}$ for the periods 1990–1992, 1993–94 and 1995. In this "eleven-parameter fit", each of the three mass values $m_{\rm Z}^{90-92}$, $m_{\rm Z}^{93-94}$ and $m_{\rm Z}^{95}$ has its specific energy error reflecting the different systematic errors on the absolute energy scale of LEP. In the combination, the relative importance of energy related and independent experimental errors on the mass values is properly treated. The input and the common energy errors, estimated in the same way as for the nine parameters, are shown in Sec. 8.3 in the appendix.

When the three values of $m_{\rm Z}$ are condensed into a single one, the effects of the time dependence of the precision in the energy calibration is taken into account. The difference of -0.2 MeV w.r.t. the $m_{\rm Z}$ value from the nine-parameter fits corresponds to 10 % of the combined error. All other parameters are identical to their values from the nine-parameter fit to within less than 5 % of the combined error. This result justifies to use the standard combination based on the nine parameters.

The averages over the four experiments of the three values $m_{\rm Z}^{90-92}$, $m_{\rm Z}^{93-94}$, $m_{\rm Z}^{95}$ also provide a cross-check on the consistency of the energy calibration, which dominates the errors on $m_{\rm Z}$ in each of the periods considered. Using the energy errors of Tab.19 allows the uncorrelated parts of the errors on the mass differences to be quantified. This is shown in Fig. 3. The differences between these values for $m_{\rm Z}$ amount to $|m_{\rm Z}^{90-92} - m_{\rm Z}^{93-94}| = 31\,\%$, $|m_{\rm Z}^{90-92} - m_{\rm Z}^{95}| = 56\,\%$ and $|m_{\rm Z}^{93-94} - m_{\rm Z}^{95}| = 43\,\%$ of the uncorrelated error, *i. e.* the three Z mass values are well consistent.

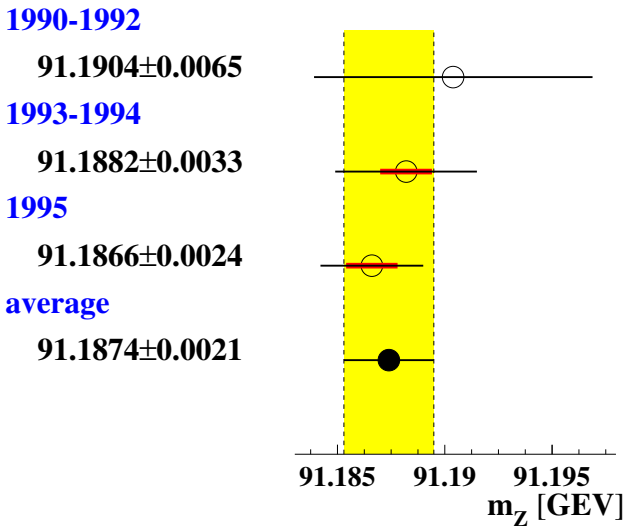

Figure 3: m_{Z} *in* GeV *for different periods of data taking, before 1993, 1993–1994 and 1995. The second, smaller error bar represents the correlated error component of* 1.2 MeV *between* m_{Z}^{93-94} *and* m_{Z}^{95}. m_{Z}^{90-92} *is essentially uncorrelated with the other two.*

6.2 Fits with lepton universality

All experiments provide fits to their measured cross-sections and asymmetries with lepton universality imposed, *i.e.* R_{e}, R_μ and R_τ are replaced by R_ℓ and $\mathrm{A}_{\mathrm{FB}}^{0,\mathrm{e}}$, $\mathrm{A}_{\mathrm{FB}}^{0,\mu}$ and $\mathrm{A}_{\mathrm{FB}}^{0,\tau}$ get replaced by $\mathrm{A}_{\mathrm{FB}}^{0,\ell}$ in the model-independent parametrisation of the differential cross-section. Here R_ℓ is defined for massless leptons. The individual experimental results and the correlation matrices are given in Tab. 18 in the appendix.

Comparing with the nine-parameter results of Tab.5, there is a noticeable change in m_{Z} of a few tenth of MeV in all experiments. This is a consequence of the dependence of the t-channel correction on m_{Z}, as discussed in Sec. 5.2. When R_{e} and $\mathrm{A}_{\mathrm{FB}}^{0,\mathrm{e}}$ are replaced by the leptonic quantities R_ℓ and $\mathrm{A}_{\mathrm{FB}}^{0,\ell}$, their correlation with the Z mass leads to a shift, which is driven by the (statistical) difference between R_{e} and R_ℓ and $\mathrm{A}_{\mathrm{FB}}^{0,\mathrm{e}}$ and $\mathrm{A}_{\mathrm{FB}}^{0,\ell}$. Similarly, replacing R_{e} and $\mathrm{A}_{\mathrm{FB}}^{0,\mathrm{e}}$ from the values of a single experiment by the LEP average introduces a shift in m_{Z} in the presence of these particular correlation coefficients. Such shifts should become smaller when averaged over the four experiments. Indeed, the average of the shifts is only -0.2 MeV.

Another aspect of the five-parameter results concerns the t-channel correction. If the average over the leptonic measurements is performed by each experiment individually, the contribution of the electron channel to R_ℓ and $\mathrm{A}_{\mathrm{FB}}^{0,\ell}$ is larger than for the case where the averages over individual lepton species are averaged at the end. This is due to the fact

that the common t-channel error becomes relatively more important for the combined data set, which leads to a reduced contribution of the electron channel to the leptonic quantities R_ℓ and $A_{FB}^{0,\ell}$. Extracting the results with lepton universality from the nine parameters is therefore the better method.

6.3 Shifts for halved experimental errors

When the average over the experiments is performed at the parameter level, information on the individual contribution of particular data points is lost. For the optimally combined data set of all four experiments, the relative importance of independent experimental errors and of common systematic errors changes, *e.g.* for data points which are dominated by experimental errors for a single experiment, but which become systematics dominated for the combined data set of the four experiments.

The examples of m_Z and the importance of the t-channel errors for R_ℓ, as discussed in the previous subsections, provide good illustrations of such effects. It was shown already in Ref. [18] that averaging the shifts in m_Z which each experiment observed when halving its experimental errors to simulate the generic "combined" experiment also reproduced the results of the full fit to the combined hadronic cross-section measurements.

While m_Z is properly treated by the eleven-parameter fits, other pseudo-observables may suffer from similar changes due to weight shifts. Changes in central values when halving the independent experimental errors in each experiment can be used as a monitoring tool. The average of these changes over the four LEP experiments serves to control the differences between an average at the parameter level compared to a full cross-section average. Of course, this assumes that all measurements from individual experiments enter into the average with the same weight. The observed shifts are summarised in Tab. 11. The shift downwards in m_Z of 0.3 MeV corresponds to the slightly smaller shift of 0.2 MeV already seen in the multiple-m_Z fits.

Thus, the average changes in m_Z, σ_h^o, R_e, $A_{FB}^{0,\mu}$ and $A_{FB}^{0,\tau}$ amount to about 10 % of the combined errors, in all other cases they are even smaller.

This cross-check provides an estimate of the magnitude of the changes in the final results that would arise from a combination at the cross-section level. The averaging at the parameter level is equal to this within at most 10 % of the combined error.

6.4 Influence of the γ–Z interference term

In the nine-parameter analyses discussed here, the γ–Z interference terms in the differential cross-sections for leptons are expressed using the effective coupling constants and the electric charges of the electron, Q^e, and the final state fermion, Q^f (see equation for the differential cross-section in Sec. 3) . For the hadronic final state, however, the γ–Z interference terms must be fixed to the SM values, as individual quark flavours are not separated. Fits with a free interference terms are possible in the S-matrix scheme [37]. A different approach was chosen by the OPAL collaboration [4] based on an extension of the standard parameter set. In the S-Matrix approach the interference terms are considered

	A	D	L	O	average	% of error
m_{Z}	-0.0006	0.0000	-0.0004	-0.0001	-0.00028	13
Γ_{Z}	-0.0002	$+0.0001$	-0.0004	0.0000	-0.00013	5
σ^o_{h}	$+0.006$	0.000	$+0.008$	$+0.0036$	$+0.0037$	10
R_{e}	$+0.004$	$+0.017$	0.000	$+0.004$	$+0.0063$	13
R_μ	0.000	0.000	0.000	$+0.001$	0.0000	0
R_τ	0.000	0.000	-0.001	$+0.002$	$+0.0003$	1
$\mathrm{A}_{\mathrm{FB}}^{0,\,\mathrm{e}}$	-0.0001	-0.0003	0.0000	-0.0000	-0.00011	5
$\mathrm{A}_{\mathrm{FB}}^{0,\,\mu}$	$+0.0002$	$+0.0003$	0.0000	$+0.0001$	$+0.00014$	11
$\mathrm{A}_{\mathrm{FB}}^{0,\,\tau}$	$+0.0002$	$+0.0003$	0.0000	$+0.0001$	$+0.00015$	9

Table 11: *Shifts in central values of the fitted pseudo-observables seen when halving the independent experimental errors, for individual experiments and average.*

as free and independent parameters. The hadronic interference term is described by the parameter $j^{\mathrm{had}}_{\mathrm{tot}}$, given in the SM by

$$j^{\mathrm{had}}_{\mathrm{tot}} = \frac{G_{\mathrm{F}} m_{\mathrm{Z}}^2}{\sqrt{2}\pi\alpha(m_{\mathrm{Z}})}\, Q^{\mathrm{e}}\, g^{\mathrm{e}}_V \times 3 \sum_{\mathrm{q}} Q^{\mathrm{q}}\, g^{\mathrm{q}}_V \,.$$

Note that the running of α as well as final state QED and QCD corrections are also included in the definition of the S-matrix parameters. The SM value of $j^{\mathrm{had}}_{\mathrm{tot}} is 0.21 \pm 0.01$.

The dependence of the nine parameters on the hadronic γ–Z interference term is studied by considering a set of ten parameters consisting of the standard nine parameters extended by the parameter $j^{\mathrm{had}}_{\mathrm{tot}}$ from the S-Matrix approach. The γ–Z interference terms in the lepton channels are fixed by the leptonic Z couplings. As already observed in S-Matrix analyses of the LEP 1 data [3], a large anti-correlation between m_{Z} and $j^{\mathrm{had}}_{\mathrm{tot}}$ appears, leading to errors on m_{Z} enlarged by a factor of almost three. The dependence of m_{Z} on $j^{\mathrm{had}}_{\mathrm{tot}}$ is given by

$$\frac{\mathrm{d}m_{\mathrm{Z}}}{\mathrm{d}j^{\mathrm{had}}_{\mathrm{tot}}} \;=\; -1.6\ \mathrm{MeV}/0.1\,.$$

The changes in all other parameters are below 20 % of their combined error for a change in $j^{\mathrm{had}}_{\mathrm{tot}}$ of 0.1 .

Better experimental constraints on the hadronic interference term are obtained by including measurements of the hadronic total cross-section at centre-of-mass energies further away from the Z pole than just the off-peak energies at LEP I. Including the measurements of the TRISTAN collaborations TOPAZ [38] and VENUS [39] at $\sqrt{(}s)$=58 GeV, the error on $j^{\mathrm{had}}_{\mathrm{tot}}$ is reduced to ± 0.1, while its central value is in good agreement with the SM expectation. Measurements at centre-of-mass energies above the Z resonance at LEP II also provide constraints on $j^{\mathrm{had}}_{\mathrm{tot}}$, but in addition test modifications to the interference terms arising from the possible existence of a heavy Z' boson [40, 41, 42, 43].

6.5 m_Z as a parameter of the Standard Model

When the set of pseudo-observables is used in the frame-work of the Standard Model, the role of m_Z changes from an independent parameter to that of a Lagrangian parameter of the theory, which now imposes additional constraints, and therefore m_Z is expected to change.

As a cross-check of the validity of the combined set of pseudo-observables as an input to Standard Model fits each collaboration provided results from direct Standard Model fits to their cross-section and asymmetry data with M_H and α_s as free parameters. The comparison of these results with those obtained by using the set of pseudo-observables as fit input instead is shown in Tab. 12. Most noticeably, a significant shift in m_Z is observed in some individual data sets, which cancels out to almost zero in the average over the four experiments. One source of this shift was already mentioned: the Z couplings defining the $\gamma - Z$ interference term depends on M_H, which is allowed to move freely in the first fit, but is fixed to 150 GeV for the extraction of the pseudo-observables. After correction for the different values of the Higgs mass given in Sec. 5.4.3 the net average difference in m_Z between the two fit procedures is less than 0.1 MeV. Shifts in the other SM parameters, in the individual data sets as well as in the average, are all well under 5 % of the errors, and therefore also negligible.

	A	D	L	O	average	% of error
χ^2/N_{df}	174/180	184/172	168/170	161/198		
m_Z [MeV]	−0.7	+0.5	0.0	+0.1	−0.03	1
M_t [GeV]	0.0	0.0	0.0	0.0	0.0	<2
$\log_{10}(M_H)$	−0.01	+0.04	+0.02	+0.04	+0.02	4
α_s	0.0000	−0.0002	+0.0002	+0.0002	+0.0001	4
$\Delta\alpha^{(5)}_{had}$	+0.00002	−0.00004	0.00000	−0.00004	−0.00002	2
fit value of M_H [GeV]	40.	10.	35.	390.		
m_Z shift [MeV] corr. to 150 GeV M_H	−0.6	+0.7	+0.1	0.0	+0.05	2

Table 12: *Shifts in SM parameters, from direct SM fit to the cross-sections and forward-backward asymmetries w.r.t. fits to the the nine-parameter results. The numbers in the lowest part of the table give the shifts in m_Z if the results from the first line are corrected to a common value of the Higgs mass of* 150 GeV.

The conclusion of this study is that SM parameters extracted from the pseudo-observables are almost identical to the ones that would be extracted from the combined cross-sections and asymmetries. Within the SM the combined set of pseudo-observables provides a description of the measurements of the Z parameters that is equivalent to the full set of cross-sections and asymmetries. This is also true for any theory beyond the SM

which leads to corrections that are absorbed in the pseudo-observables. An exception to this are those theories with an additional Z′-bosons which have significant modifications of the $\gamma - \mathrm{Z}$ interference term, because the nine pseudo-observables are derived under the assumption that this is given by only the photon and Z-boson couplings.

6.6 Combined results

The result of the combination of the four sets of nine pseudo-observables including the experimental and common error matrices, as shown in Tab. 10, is given in Tab. 13. The value of the Higgs boson mass was assumed to be 150 GeV and is relevant only for the value of m_{Z}, which changes by +0.23 MeV per unit change in $\log_{10}(M_{\mathrm{H}}/\mathrm{GeV})$.

without lepton universality		correlations							
$\chi^2/N_{\mathrm{df}} = 32.6/27$									
m_{Z} [GeV]	91.1876± 0.0021	1.00	-.024	-.044	.078	.000	.002	-.014	.046	.035
Γ_{Z} [GeV]	2.4952 ± 0.0023	-.024	1.00	-.297	-.011	.008	.006	.007	.002	.001
σ^o_{h} [nb]	41.541 ± 0.037	-.044	-.297	1.00	.105	.131	.092	.001	.003	.002
R_{e}	20.804 ± 0.050	.078	-.011	.105	1.00	.069	.046	-.371	.020	.013
R_μ	20.785 ± 0.033	.000	.008	.131	.069	1.00	.069	.001	.012	-.003
R_τ	20.764 ± 0.045	.002	.006	.092	.046	.069	1.00	.003	.001	.009
$\mathrm{A}^{0,\mathrm{e}}_{\mathrm{FB}}$	0.0145 ± 0.0025	-.014	.007	.001	-.371	.001	.003	1.00	-.024	-.020
$\mathrm{A}^{0,\mu}_{\mathrm{FB}}$	0.0169 ± 0.0013	.046	.002	.003	.020	.012	.001	-.024	1.00	.046
$\mathrm{A}^{0,\tau}_{\mathrm{FB}}$	0.0188 ± 0.0017	.035	.001	.002	.013	-.003	.009	-.020	.046	1.00
with lepton universality										
$\chi^2/N_{\mathrm{df}} = 36.5/31$										
m_{Z} [GeV]	91.1875± 0.0021	1.00	-.023	-.045	.033	.055				
Γ_{Z} [GeV]	2.4952 ± 0.0023	-.023	1.00	-.297	.004	.003				
σ^o_{h} [nb]	41.540 ± 0.037	-.045	-.297	1.00	.183	.006				
R_ℓ	20.767 ± 0.025	.033	.004	.183	1.00	-.056				
$\mathrm{A}^{0,\ell}_{\mathrm{FB}}$	0.01714 ± 0.00095	.055	.003	.006	-.056	1.00				

Table 13: *Result of the combination of the four sets of nine pseudo-observables by the* LEP *experiments.* **Due to the OPAL input not yet being approved for publication, this average has still to be considered as preliminary.**

The value of χ^2 per degree of freedom of the combination is 32.6/27 and corresponds to a probability of 21 % to find an agreement among the four sets of measurements which is worse than the one actually observed. The correlation matrix of the combined result shows significant correlations of σ^o_{h} with Γ_{Z} and R_{e}, R_μ and R_τ and between R_{e} and $\mathrm{A}^{0,\mathrm{e}}_{\mathrm{FB}}$.

A comparison of the leptonic quantites R_{e}, R_μ and R_τ and of $\mathrm{A}^{0,\mathrm{e}}_{\mathrm{FB}}$, $\mathrm{A}^{0,\mu}_{\mathrm{FB}}$ and $\mathrm{A}^{0,\tau}_{\mathrm{FB}}$ shows that they agree within errors. [5] Fig. 4 shows the corresponding 68 % level contours in the R_ℓ–$\mathrm{A}^{0,\ell}_{\mathrm{FB}}$ plane.

[5] Note that R_τ is expected to be larger by 0.023 % because of τ mass effects.

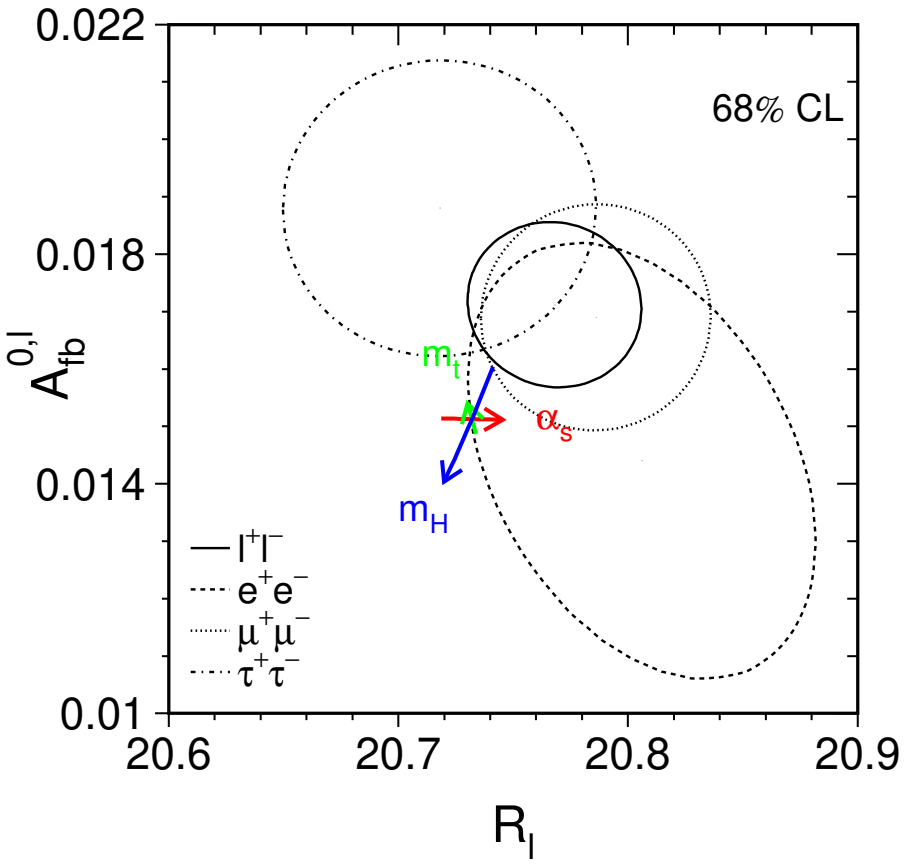

Figure 4: *Contour lines (68 % CL) in the* R_ℓ–$A_{FB}^{0,\ell}$ *plane, for* e^+e^-, $\mu^+\mu^-$ *and* $\tau^+\tau^-$ *final states and for all leptons combined.*

Imposing the additional requirement of lepton universality in the combination leads to the results shown in the second part of Tab. 13. The value of χ^2/N_{df} of 36.5/31 for the combination of the four sets of nine pseudo-observables into the five parameters of Tab. 13 corresponds to a χ^2-probability of 23 %. The central ellipse in Fig. 4 shows the 68 %-CL contour for the combined values of R_ℓ and $A_{FB}^{0,\ell}$ determined from all three lepton species.

In principle, the average over the four experiments can also be performed at the level of the five parameter results of Sec. 6.2. Good agreement is seen with the results in the lower part of Tab. 13 except for R_ℓ, where the difference amounts to 0.005 or 20 % of the total error. The origin of this shift is the common t-channel error, as discussed in Sec. 6.2 above.

6.7 Parameter Transformations

By parameter transformation some more familiar pseudo-observables than the experimentally motivated set of Tab. 13 is obtained. The partial Z decay widths are summarised in Tab. 14. Note that they represent a highly correlated set of results. If lepton universality is imposed, a more precise value of $\Gamma_{\rm had}$ is obtained, because $\Gamma_{\rm ee}$ in the relation between the hadronic pole cross-section and the partial widths is replaced by the more precise value of $\Gamma_{\ell\ell}$. The invisible width, $\Gamma_{\rm inv} = \Gamma_{\rm Z} - \Gamma_{\rm had} - \Gamma_{\rm ee} - \Gamma_{\mu\mu} - \Gamma_{\tau\tau}$, is also shown in the table. The leptonic pole cross-section, σ^o_ℓ, defined as

$$\sigma^o_\ell \equiv \frac{12\pi}{m^2_{\rm Z}} \frac{\Gamma^2_{\ell\ell}}{\Gamma^2_{\rm Z}},$$

in analogy to $\sigma^o_{\rm h}$, is shown in the last line of Tab.14. Because α_s appears quadratically in the denominator via $\Gamma_{\rm Z}$, σ^o_ℓ has a higher sensitivity to α_s than $\sigma^o_{\rm h}$ or R_ℓ, where the dependence on α_s is only linear.

	without lepton universality	correlation matrix			
$\Gamma_{\rm had}$ [MeV]	1745.8±2.7	1.00	-0.29	0.66	0.54
$\Gamma_{\rm ee}$ [MeV]	83.92 ±0.12	-0.29	1.00	-0.20	-0.17
$\Gamma_{\mu\mu}$ [MeV]	83.99 ±0.18	0.66	-0.20	1.00	0.39
$\Gamma_{\tau\tau}$ [MeV]	84.08 ±0.22	0.54	-0.17	0.39	1.00

	with lepton universality			
$\Gamma_{\rm inv}$ [MeV]	499.0±1.5	1.00	-0.29	0.49
$\Gamma_{\rm had}$ [MeV]	1744.4±2.0	-0.29	1.00	0.39
$\Gamma_{\ell\ell}$ [MeV]	83.984±0.086	0.49	0.39	1.00
$\Gamma_{\rm inv}/\Gamma_{\ell\ell}$	5.942±0.016			
σ^o_ℓ [nb]	2.0003±0.0027			

Table 14: *Partial* Z *decay widths and error correlation matrix.*

Assuming only standard particles, the invisible width is compatible with the SM hypothesis of decays into the three neutrino species, $\Gamma_{\rm inv} = 3\,\Gamma_{\nu\nu}$. As a check, the "number of neutrinos" N_ν is calculated according to

$$\frac{\Gamma_{\rm inv}}{\Gamma_{\ell\ell}} = N_\nu \left(\frac{\Gamma_{\nu\nu}}{\Gamma_{\ell\ell}}\right)_{\rm SM}.$$

The Standard Model value for the ratio of the partial widths to neutrinos and to charged leptons is 1.9912±0.0012, where the uncertainty arises from variations of the top quark mass within its experimental error and of the Higgs mass within 100 GeV $< M_{\rm H} <$ 1000 GeV.

With the measured value of $\Gamma_{\rm inv} \,/\, \Gamma_{\ell\ell} = 5.942 \pm 0.016$, the number of light neutrino species becomes

$$N_\nu = 2.984 \pm 0.008 \; .$$

This may also be turned into a quantitative limit on extra, non-standard contributions to the invisible width, *i. e.* not originating from $\mathrm{Z} \to \nu\overline{\nu}$, by taking the difference between the value given in Tab. 14 and the Standard Model expectation of $(\Gamma_{\rm inv})_{\rm SM} = 501.7^{+0.1}_{-0.9}\,\mathrm{MeV}$. This gives $\Gamma^x_{\rm inv} = -2.7^{+1.7}_{-1.5}\,\mathrm{MeV}$, or expressed as a limit, $\Delta\Gamma^x_{\rm inv} < 2.0\,\mathrm{MeV}$ @ 95% CL; here, the limit was conservatively calculated allowing only positive values of $\Gamma^x_{\rm inv}$.

The leptonic pole asymmetry, $\mathrm{A}^{0,\,\ell}_{\rm FB}$, depends only on the ratio of the universal lepton couplings $g^\ell_V \,/\, g^\ell_A$, as is easily seen from its definition given in Sec. 3. The effective weak mixing angle is related to the ratio of the leptonic couplings by

$$\sin^2\theta^{\rm lept}_{eff} \;=\; \frac{1}{4}\left(1 \,-\, \frac{g^\ell_V}{g^\ell_A}\right) \; .$$

$\mathrm{A}^{0,\,\ell}_{\rm FB}$ therefore directly determines $\sin^2\theta^{\rm lept}_{eff}$, if the sign of the ratio of couplings is chosen to be positive, in agreement with studies of the polarisation of τ leptons at LEP. Thus the combined value of $\mathrm{A}^{0,\,\ell}_{\rm FB} = 0.01714 \pm 0.00095$ results in $\sin^2\theta^{\rm lept}_{eff} = 0.23099 \pm 0.00053$.

7 Conclusion

The combination procedure adopted by the LEP electroweak working group for the set of pseudo-observables derived from the measured hadronic and leptonic cross-sections and the leptonic forward-backward asymmetries at centre-of-mass energies around the Z resonance has been described.

Detailed studies of common systematic errors were performed. The dominant contribution of $\pm 1.7\,\mathrm{MeV}$ to the combined error on the Z mass arises from the calibration of the energy of the beams in LEP. The dominant contribution of $\pm 0.025\,\mathrm{nb}$ to the uncertainty on the hadronic cross-section at the pole of the Z resonance arises from the theoretical error on the small-angle Bhabha cross-section. The errors on all other parameters are dominated by independent experimental or statistical errors.

The combined LEP results on the mass and width of the Z, on the hadronic pole cross-section, on the ratio of the hadronic and leptonic partial width and on the pole forward-backward asymmetry are

$$\begin{array}{lrcl}
m_{\rm Z} & = & 91.1875 & \pm \; 0.0021\,\mathrm{GeV}\,, \\
\Gamma_{\rm Z} & = & 2.4952 & \pm \; 0.0023\,\mathrm{GeV}\,, \\
\sigma^o_{\rm h} & = & 41.540 & \pm \; 0.037\,\mathrm{nb}\,, \\
R_\ell & = & 20.767 & \pm \; 0.025\,, \\
\mathrm{A}^{0,\,\ell}_{\rm FB} & = & 0.01714 & \pm \; 0.00095\,.
\end{array}$$

There are significant correlations above 5 % only between $\sigma^o_{\rm h}$ and $\Gamma_{\rm Z}$ of -30 % and between $\sigma^o_{\rm h}$ and R_ℓ of 19 %. The full set of results and the error correlation matrices are shown in Tab. 13.

The technical precision of the central values is estimated to be within 5 % of the combined error. The combination procedure approximates a statistically optimal average based on the measured cross-sections and forward-backward asymmetries to within at least 10 % of the combined errors. Using the combined parameter set in the framework of the minimal Standard Model yields results which are identical to within 5 % of the combined errors to those which would be obtained directly from the measured cross-sections and asymmetries.

ACKNOWLEDGEMENTS

We wish to thank the CERN SL division for the excellent performance of the LEP collider, and the working group on energy calibration for providing a precise knowledge on the beam energies. We would also like to thank all our theorist colleagues who have contributed to the calculations of electroweak physics, and the TOPAZ0 and ZFITTER teams who have incorporated these calculations and made them available to us.

8 Appendix

8.1 Common errors estimated by individual experiments

		m_{Z}	Γ_{Z}	σ^o_{h}	R_{e}
ALEPH	m_{Z}	0.0017			
	Γ_{Z}	−0.0004	0.0012		
	σ^o_{h}	−0.0028	−0.0024	0.011	
	R_{e}	0.0013	−0.0015	0.007	0.012
DELPHI	m_{Z}	0.0016			
	Γ_{Z}	−0.0005	0.0012		
	σ^o_{h}	−0.0025	−0.0024	0.009	
	R_{e}	0.0014	0.0000	0.004	0.016
L3	m_{Z}	0.0016			
	Γ_{Z}	−0.0008	0.0013		
	σ^o_{h}	−0.0009	−0.0030	0.011	
	R_{e}	0.0020	−0.0021	0.010	0.013
OPAL	m_{Z}	0.0017			
	Γ_{Z}	−0.0005	0.0012		
	σ^o_{h}	−0.0011	−0.0028	0.011	
	R_{e}	0.0019	−0.0019	0.008	0.012

Table 15: *Common energy errors, from individual data sets for the nine-parameter fits. Values are given as the signed square root of the covariance matrix elements; elements above the diagonal have been omitted for simplicity.*

		$A_{FB}^{0,e}$	$A_{FB}^{0,\mu}$	$A_{FB}^{0,\tau}$
ALEPH	$A_{FB}^{0,e}$	0.0003		
	$A_{FB}^{0,\mu}$	−0.0003	0.0003	
	$A_{FB}^{0,\tau}$	−0.0003	0.0003	0.0003
DELPHI	$A_{FB}^{0,e}$	0.0004		
	$A_{FB}^{0,\mu}$	−0.0003	0.0003	
	$A_{FB}^{0,\tau}$	−0.0003	0.0003	0.0003
L3	$A_{FB}^{0,e}$	0.0003		
	$A_{FB}^{0,\mu}$	−0.0002	0.0003	
	$A_{FB}^{0,\tau}$	−0.0002	0.0002	0.0003
OPAL	$A_{FB}^{0,e}$	0.0004		
	$A_{FB}^{0,\mu}$	−0.0003	0.0003	
	$A_{FB}^{0,\tau}$	−0.0003	0.0003	0.0003

Table 16: *Common energy errors for forward-backward asymmetries, estimated from the data sets of individual experiments.*

		R_e	$A_{FB}^{0,e}$
ALEPH	R_e	0.025	
	$A_{FB}^{0,e}$	−0.0056	0.0013
DELPHI	R_e	0.025	
	$A_{FB}^{0,e}$	−0.0058	0.0016
L3	R_e	0.021	
	$A_{FB}^{0,e}$	−0.0046	0.0010
OPAL	R_e	0.025	
	$A_{FB}^{0,e}$	−0.0057	0.0015

Table 17: *Estimates of the t-channel errors of individual experiments and average, for ALIBABA.*

8.2 Results with lepton universality

$\chi^2/N_{\rm df}$ = 172/180		ALEPH				
$m_{\rm Z}$ [GeV]	91.1893 ± 0.0031	1.00	.038	-.092	.033	.071
$\Gamma_{\rm Z}$ [GeV]	2.4959 ± 0.0043	.038	1.00	-.383	.011	.002
$\sigma^o_{\rm h}$ [nb]	41.559 ± 0.057	-.092	-.383	1.00	.246	.001
R_ℓ	20.729 ± 0.039	.033	.011	.246	1.00	-.076
$A^{0,\ell}_{\rm FB}$	0.0173 ± 0.0016	.071	.002	.001	-.076	1.00

$\chi^2/N_{\rm df}$ = 183/172		DELPHI				
$m_{\rm Z}$ [GeV]	91.1863 ± 0.0028	1.00	.046	-.070	.028	.095
$\Gamma_{\rm Z}$ [GeV]	2.4876 ± 0.0041	.046	1.00	-.270	-.006	.006
$\sigma^o_{\rm h}$ [nb]	41.578 ± 0.069	-.070	-.270	1.00	.242	-.005
R_ℓ	20.730 ± 0.060	.028	-.006	.242	1.00	.000
$A^{0,\ell}_{\rm FB}$	0.0187 ± 0.0019	.095	.006	-.005	.000	1.00

$\chi^2/N_{\rm df}$ = 163/170		L3				
$m_{\rm Z}$ [GeV]	91.1894 ± 0.0030	1.00	.068	.014	.067	.041
$\Gamma_{\rm Z}$ [GeV]	2.5025 ± 0.0041	.068	1.00	-.348	.020	.020
$\sigma^o_{\rm h}$ [nb]	41.536 ± 0.055	.014	-.348	1.00	.111	.005
R_ℓ	20.809 ± 0.060	.067	.020	.111	1.00	-.024
$A^{0,\ell}_{\rm FB}$	0.0192 ± 0.0024	.041	.020	.005	-.024	1.00

$\chi^2/N_{\rm df}$ = 158/198		OPAL				
$m_{\rm Z}$ [GeV]	91.1853 ± 0.0029	1.00	.051	.030	.043	.075
$\Gamma_{\rm Z}$ [GeV]	2.4947 ± 0.0041	.051	1.00	-.352	.024	-.005
$\sigma^o_{\rm h}$ [nb]	41.502 ± 0.055	.030	-.352	1.00	.290	.013
R_ℓ	20.822 ± 0.044	.043	.024	.290	1.00	-.017
$A^{0,\ell}_{\rm FB}$	0.0145 ± 0.0017	.075	-.005	.013	-.017	1.00

Table 18: *Results on Z parameters and error correlation matrices by the four experiments with lepton universality imposed.*

8.3 Results from eleven-parameter fits

ALEPH

Γ_{Z} [GeV]	2.4957 ± 0.0043
σ^{o}_{h} [nb]	41.559 ± 0.057
R_{e}	20.694 ± 0.075
R_{μ}	20.801 ± 0.056
R_{τ}	20.709 ± 0.062
$\mathrm{A}_{\mathrm{FB}}^{0,\,\mathrm{e}}$	0.0184 ± 0.0034
$\mathrm{A}_{\mathrm{FB}}^{0,\,\mu}$	0.0173 ± 0.0025
$\mathrm{A}_{\mathrm{FB}}^{0,\,\tau}$	0.0171 ± 0.0028
m_{Z}^{90-92} [GeV]	91.1928 ± 0.0092
m_{Z}^{93-94} [GeV]	91.1926 ± 0.0046
m_{Z}^{95} [GeV]	91.1852 ± 0.0043

correlation matrix

1.000	-0.384	0.001	0.012	0.003	0.001	0.000	0.000	0.015	-0.011	0.055
-0.384	1.000	0.137	0.167	0.152	-0.004	0.003	0.003	-0.043	-0.037	-0.074
0.001	0.137	1.000	0.083	0.067	-0.389	0.020	0.017	0.063	0.063	0.036
0.012	0.167	0.083	1.000	0.093	0.000	0.014	0.000	0.003	-0.001	-0.004
0.003	0.152	0.067	0.093	1.000	0.000	0.000	0.012	0.001	-0.001	-0.004
0.001	-0.004	-0.389	0.000	0.000	1.000	-0.009	-0.008	-0.037	-0.036	-0.020
0.000	0.003	0.020	0.014	0.000	-0.009	1.000	0.018	0.056	0.063	0.022
0.000	0.003	0.017	0.000	0.012	-0.008	0.018	1.000	0.045	0.060	0.018
0.015	-0.043	0.063	0.003	0.001	-0.037	0.056	0.045	1.000	0.016	0.011
-0.011	-0.037	0.063	-0.001	-0.001	-0.036	0.063	0.060	0.016	1.000	0.093
0.055	-0.074	0.036	-0.004	-0.004	-0.020	0.022	0.018	0.011	0.093	1.000

DELPHI

Γ_{Z} [GeV]	2.4878 ± 0.0041
σ^{o}_{h} [nb]	41.573 ± 0.069
R_{e}	20.88 ± 0.12
R_{μ}	20.650 ± 0.076
R_{τ}	20.84 ± 0.13
$\mathrm{A}_{\mathrm{FB}}^{0,\,\mathrm{e}}$	0.0170 ± 0.0049
$\mathrm{A}_{\mathrm{FB}}^{0,\,\mu}$	0.0164 ± 0.0025
$\mathrm{A}_{\mathrm{FB}}^{0,\,\tau}$	0.0240 ± 0.0037
m_{Z}^{90-92} [GeV]	91.1883 ± 0.0084
m_{Z}^{93-94} [GeV]	91.1824 ± 0.0043
m_{Z}^{95} [GeV]	91.1894 ± 0.0038

correlation matrix

1.000	-0.271	-0.001	-0.007	-0.001	-0.001	0.005	0.003	0.002	0.012	0.062
-0.271	1.000	0.123	0.191	0.113	-0.003	0.002	0.001	-0.003	0.015	-0.066
-0.001	0.123	1.000	0.054	0.033	-0.105	0.027	0.016	0.055	0.044	0.029
-0.007	0.191	0.054	1.000	0.051	0.000	0.008	0.000	0.000	-0.002	-0.002
-0.001	0.113	0.033	0.051	1.000	-0.001	0.000	0.011	-0.001	-0.001	0.002
-0.001	-0.003	-0.105	0.000	-0.001	1.000	-0.014	-0.014	0.048	0.052	0.016
0.005	0.002	0.027	0.008	0.000	-0.014	1.000	0.015	0.057	0.053	0.021
0.003	0.001	0.016	0.000	0.011	-0.014	0.015	1.000	0.032	0.037	0.016
0.002	-0.003	0.055	0.000	-0.001	0.048	0.057	0.032	1.000	0.016	0.007
0.012	0.015	0.044	-0.002	-0.001	0.052	0.053	0.037	0.016	1.000	0.088
0.062	-0.066	0.029	-0.002	0.002	0.016	0.021	0.016	0.007	0.088	1.000

L3	
Γ_{Z} [GeV]	2.5024 ± 0.0041
σ^{o}_{h} [nb]	41.540 ± 0.055
R_{e}	20.821 ± 0.089
R_{μ}	20.861 ± 0.097
R_{τ}	20.79 ± 0.13
$\mathrm{A}^{0,\mathrm{e}}_{\mathrm{FB}}$	0.0106 ± 0.0058
$\mathrm{A}^{0,\mu}_{\mathrm{FB}}$	0.0190 ± 0.0033
$\mathrm{A}^{0,\tau}_{\mathrm{FB}}$	0.0261 ± 0.0047
m_{Z}^{90-92} [GeV]	91.1973 ± 0.0092
m_{Z}^{93-94} [GeV]	91.1912 ± 0.0047
m_{Z}^{95} [GeV]	91.1870 ± 0.0041

correlation matrix

1.000	-0.354	-0.001	-0.001	0.004	-0.002	-0.001	0.000	0.017	0.014	0.072
-0.354	1.000	0.081	0.078	0.055	0.011	0.011	0.007	0.087	0.022	-0.038
-0.001	0.081	1.000	0.030	0.024	-0.150	0.020	0.014	0.117	0.050	0.059
-0.001	0.078	0.030	1.000	0.020	-0.002	0.005	-0.000	0.002	-0.001	-0.001
0.004	0.055	0.024	0.020	1.000	-0.004	-0.000	0.009	0.002	0.001	0.002
-0.002	0.011	-0.150	-0.002	-0.004	1.000	0.011	-0.007	-0.044	-0.016	-0.037
-0.001	0.011	0.020	0.005	-0.000	0.011	1.000	0.007	0.051	0.047	0.010
0.000	0.007	0.014	-0.000	0.009	-0.007	0.007	1.000	0.025	0.034	0.008
0.017	0.087	0.117	0.002	0.002	-0.044	0.051	0.025	1.000	0.004	0.002
0.014	0.022	0.050	-0.001	0.001	-0.016	0.047	0.034	0.004	1.000	0.083
0.072	-0.038	0.059	-0.001	0.002	-0.037	0.010	0.008	0.002	0.083	1.000

OPAL	
Γ_{Z} [GeV]	2.4946 ± 0.0042
σ^{o}_{h} [nb]	41.506 ± 0.057
R_{e}	20.903 ± 0.085
R_{μ}	20.812 ± 0.058
R_{τ}	20.833 ± 0.091
$\mathrm{A}^{0,\mathrm{e}}_{\mathrm{FB}}$	0.0089 ± 0.0045
$\mathrm{A}^{0,\mu}_{\mathrm{FB}}$	0.0159 ± 0.0023
$\mathrm{A}^{0,\tau}_{\mathrm{FB}}$	0.0146 ± 0.0030
m_{Z}^{90-92} [GeV]	91.1851 ± 0.0091
m_{Z}^{93-94} [GeV]	91.1872 ± 0.0046
m_{Z}^{95} [GeV]	91.1849 ± 0.0039

correlation matrix

1.000	-0.369	0.001	0.019	0.012	-0.002	-0.009	-0.007	0.002	-0.065	0.107
-0.369	1.000	0.164	0.218	0.137	0.005	0.018	0.014	0.009	0.185	-0.100
0.001	0.164	1.000	0.090	0.042	-0.228	0.034	0.026	0.079	0.106	0.032
0.019	0.218	0.090	1.000	0.058	-0.002	0.012	-0.001	-0.007	0.005	0.000
0.012	0.137	0.042	0.058	1.000	0.000	0.000	0.016	-0.007	0.007	-0.001
-0.002	0.005	-0.228	-0.002	0.000	1.000	-0.017	-0.013	-0.040	-0.046	-0.021
-0.009	0.018	0.034	0.012	0.000	-0.017	1.000	0.019	0.062	0.073	0.024
-0.007	0.014	0.026	-0.001	0.016	-0.013	0.019	1.000	0.045	0.058	0.019
0.002	0.009	0.079	-0.007	-0.007	-0.040	0.062	0.045	1.000	0.021	0.006
-0.065	0.185	0.106	0.005	0.007	-0.046	0.073	0.058	0.021	1.000	0.093
0.107	-0.100	0.032	0.000	-0.001	-0.021	0.024	0.019	0.006	0.093	1.000

The common energy errors are shown in Tab. 19. The agreement of the energy-related errors for the eleven parameter results is acceptable among the experiments. Noticeable are the differences in the covariance matrix elements between the Z mass values and σ^{o}_{h}. They were traced back to a slightly different treatment of the role of m_{Z} when transforming the hadronic pole cross-section into the partial widths Γ_{ee} and Γ_{had}, which are used in the fit programs to parametrise the differential cross-sections around the Z resonance.

		$\Gamma_{\rm Z}$	$\sigma^o_{\rm h}$	$R_{\rm e}$	$m_{\rm Z}^{90-92}$	$m_{\rm Z}^{93-94}$	$m_{\rm Z}^{95}$
ALEPH	$m_{\rm Z}^{90-92}$	−0.0011	−0.002	0.0020	0.0058		
	$m_{\rm Z}^{93-94}$	−0.0007	−0.003	0.0016	0.0006	0.0028	
	$m_{\rm Z}^{95}$	0.0002	−0.002	0.0003	0.0003	0.0013	0.0015
DELPHI	$m_{\rm Z}^{90-92}$	−0.0009	0.0014	0.0027	0.0053		
	$m_{\rm Z}^{93-94}$	−0.0006	−0.0020	0.0014	0.0008	0.0027	
	$m_{\rm Z}^{95}$	−0.0002	−0.0018	0.0007	0.0004	0.0012	0.0014
L3	$m_{\rm Z}^{90-92}$	−0.0013	0.0045	0.0046	0.0050		
	$m_{\rm Z}^{93-94}$	−0.0007	−0.0022	−0.0007	−0.0008	0.0028	
	$m_{\rm Z}^{95}$	−0.0001	−0.0018	−0.0006	−0.0009	0.0012	0.0015
OPAL	$m_{\rm Z}^{90-92}$	−0.0011	0.0025	0.0036	0.0058		
	$m_{\rm Z}^{93-94}$	−0.0010	0.0034	0.0034	0.0006	0.0030	
	$m_{\rm Z}^{95}$	0.0000	−0.0014	0.0013	−0.0003	0.0012	0.0015
average	$m_{\rm Z}^{90-92}$	−0.0011	0.0016	0.0032	0.0055		
	$m_{\rm Z}^{93-94}$	−0.0008	−0.0010	0.0014	0.0003	0.0028	
	$m_{\rm Z}^{95}$	0.0000	−0.0018	−0.0004	−0.0001	0.0012	0.0015

Table 19: *Common energy errors for multiple-$m_{\rm Z}$ fit, from individual data sets and average. The matrix elements for $\Gamma_{\rm Z}$, $\sigma^o_{\rm h}$ and $R_{\rm e}$ and for the asymmetries are very similar to the nine-parameter case and can be taken from Tab. 15 and 16.*

References

[1] ALEPH Coll. (D. Decamp *et al.*), Z. Phys. **C48** (1990) 365;
Z. Phys. **C53** (1992) 1;
ALEPH Coll., (D. Buskulic *et al.*), Z. Phys. **C60** (1993) 71;
Z. Phys. **C62** (1994) 539;
ALEPH Coll., (R. Barate *et al.*), Europ. Phys. J. **C 14** (2000) 1.

[2] DELPHI Coll. (P. Aarnio *et al.*), Nucl. Phys. **B367** (1991) 511;
DELPHI Coll. (P. Abreu *et al.*), Nucl. Phys. **B417** (1994) 3;
Nucl. Phys. **B418** (1994) 403;
Cross-Sections and Leptonic Forward-Backward Asymmetries from the Z *Running of LEP*, CERN-EP-2000-037, accepted for publication by Europ. Phys. J. **C**.

[3] L3 Coll. (B. Adeva *et al.*), Z. Phys. **C51** (1991) 179;
L3 Coll. (O. Adriani *et al.*), Phys. Rep. **236** (1993) 1;
L3 Coll. (M. Acciarri *et al.*), Z. Phys. **C62** (1994) 551;
Measurement of Cross Sections and Forward-Backward Asymmetries at the Z Resonance and Determination of Electroweak Parameters, CERN-EP-2000-022, accepted for publication by Europ. Phys. J. **C**.

[4] OPAL Coll. (G. Alexander *et al.*), Z. Phys. **C52** (1991) 175;
OPAL Coll. (P.D. Acton *et al.*), Z. Phys. **C58** (1993) 219;
OPAL Coll. (R. Akers *et al.*), Z. Phys. **C61** (1994) 19;
OPAL Coll., *Precision Measurements of the Z^0 Lineshape and Lepton Asymmetry*, OPAL Physics Note PN358, July 1998;
OPAL Coll., *Update to Precision Measurements of the Z0 Lineshape and Lepton Asymmetry*, OPAL Physics Note PN404, July 1999;
OPAL Coll. (G. Abbiendi *et al.*), *Precision Luminosity for Z0 Lineshape Measurements with a Silicon-Tungsten Calorimeter*, Eur. Phys. J. **C14** (2000) 373;
OPAL Coll., *Update to Precision Measurements of the Z0 Lineshape and Lepton Asymmetry*, OPAL Physics Note PN442, July 2000.

[5] *Z Physics at LEP1*, CERN 89-08, ed. G. Altarelli *et al.*, Vol. 1–3 (1989) and references therein.

[6] ALEPH Coll. (D. Decamp *et al.*), Nucl. Inst. Meth. **A294** (1990) 121;
ALEPH Coll. (D. Buskulic *et al.*), Nucl. Inst. Meth. **A360** (1995) 481-506.

[7] DELPHI Coll. (P. Aarnio *et al.*), Nucl. Inst. Meth. **A303** (1991) 233;
(P. Abreu *et al.*), Nucl. Inst. Meth. **A378** (1996) 57-100.

[8] L3 Coll. (B. Adeva *et al.*), Nucl. Inst. Meth. **A289** (1990) 35;
L3 Coll. (M. Acciarri *et al.*), Nucl. Inst. Meth. **A351** (1994) 300;
L3 Coll. (M. Chemarin *et al.*), Nucl. Inst. Meth. **A349** (1994) 345;

L3 Coll. (A. Adam *et al.*), Nucl. Inst. Meth. **A383** (1996) 342;
L3 Coll. (I.C. Brock *et al.*), Nucl. Inst. Meth. **A381** (1996) 236.

[9] OPAL Coll. (K. Ahmet *et al.*), Nucl. Inst. Meth. **A305** (1991) 275;
OPAL Coll. (P. Allport *et al.*), Nucl. Inst. Meth. **A324** (1993) 34;
OPAL Coll. (P. Allport *et al.*), Nucl. Inst. Meth. **A346** (1994) 476;
OPAL Coll. (B.E. Anderson *et al.*), IEEE Trans. Nucl. Sci. **41** (1994) 845.

[10] The LEP Collaborations ALEPH, DELPHI, L3 and OPAL and the LEP Electroweak working group (Abbaneo D. *et al.*), *A Combination of Preliminary Electroweak Measurements and Constraints on the Standard Model*, CERN-EP/2000-016.

[11] The working group on LEP energy and the Collaborations ALEPH, DELPHI, L3 and OPAL, Phys. Lett. **B307** (1993) 187–193.

[12] Working group on LEP energy (L. Arnaudon *et al.*), *The Energy Calibration of LEP in 1992*, CERN SL/93-21 (DI), April 1993.

[13] Working group on LEP energy (R. Assmann *et al.*), *The energy calibration of LEP in the 1993 scan*, Z. Phys. **C66** (1995) 567-582.

[14] Working group on LEP energy (R. Billen *et al.*), *Calibration of Centre-of-Mass Energies at LEP1 for Precise Measurements of Z properties*, Eur. Phys. J. **C6** (1999) 187.

[15] G. Montagna, O. Nicrosini, G. Passarino, F. Piccinni and R. Pittau, Nucl. Phys. **B401** (1993) 3; Comp. Phys. Comm. **76** (1993) 328; Comp. Phys. Comm. **93** (1996) 120;
G. Montagna, O. Nicrosini, G. Passarino and F. Piccinini, hep-ph/9804211, recently updated to include initial state pair radiation (G. Passarino, priv. comm.).

[16] D. Bardin *et al.*, Z. Phys. **C44** (1989) 493;
Comp. Phys. Comm. **59** (1990) 303;
Nucl. Phys. **B351** (1991) 1;
Phys. Lett. **B255** (1991) 290 and CERN-TH 6443/92 (May1992);
DESY Report 99-070, hep-ph/9908433 (Aug. 1999); recently updated with results from [36], accepted for publication by Comp. Phys. Comm.

[17] D. Bardin, G. Passarino, *Upgrading of Precision Calculations for Electroweak Observables*, hep-ph/9803425 ;
D. Bardin, G. Passarino and M. Grünewald, *Precision Calculation Project Report*, hep-ph/9902452 .

[18] G. Duckeck, R. Kellogg, A. Olshevski, C. Paus, G. Quast, P. Renton and D. Strom (LEP EWWG: the m_Z and Γ_Z task force), *Precise Determination of Z–Boson Mass and Width at LEP*, LEPEWWG/LS 98-01.

[19] W.Beenakker, F.A.Berends and S.C. van der Marck, Nucl. Phys. **B349** (1991) 323.

[20] W.Beenakker and G.Passarino, Phys. Letters **B425** (1998) 199-207.

[21] W.Beenakker and G.Passarino, private communications.

[22] S. Jadach *et al.*, BHLUMI 4.04, Comp. Phys. Comm. **102** (1997) 229;
S. Jadach and O. Nicrosini, *Event generators for Bhabha scattering*, in *Physics at LEP2*, CERN 96-01 Vol. 2, February 1996.

[23] B.F.L Ward *et al.*, *New Results on the Theoretical Precision of the LEP/SLC Luminosity*, UTHEP-96-501 (1998), Proceedings of the 29th International Conference on High Energy Physics, Vancouver, Canada (23-29 July 1998) 425.

[24] G. Montagna *et al.*, Phys.Lett. **B459** (1999) 649-652.

[25] F.A. Berends, W.L. van Neerven and G.J.H. Burgers, Nucl. Phys. **B297** (1988) 429 and **B304** (1988) 921 (E).

[26] E.A. Kuraev and V.S.Fadin, Sov. J. Nucl. Phys. **41** (1985) 466.

[27] G. Montagna, O. Nicrosini and F. Piccinini, Phys. Lett. **B406** (1997) 243.

[28] M. Skrzypek, Acta Phys. Polonica, **B23** (1992) 135.

[29] S. Jadach, M. Skrzypek and B.F.L. Ward, Phys. Lett. **B257** (1991) 173.

[30] D.R. Yennie, S.C. Frautschi and H. Suura, Ann. Phys. (NY) **13** (1961) 379.

[31] S.Jadach, B.Pietrzyk and M. Skrzypek, Phys. Lett. **B456** (1999) 77.

[32] L. Garrido *et al.*, Z. Phys. **C49** (1991) 645;
M. Martinez and F. Teubert, Z. Phys. **C65** (1995) 267, updated with results summarized in [31] and [44].

[33] S. Jadach, B. Pietrzyk, E. Tournefier, B.F.L. Ward and Z. Wąs, Phys. Lett. **B465** (1999) 254.

[34] B.A. Kniehl *et al.*, Phys. Lett. **B 209** (1988) 337.

[35] S. Jadach, M. Skrzypek and M. Martinez, Phys. Lett. **B280** (1992) 129.

[36] A.B. Arbuzov, *Light pair corrections to electron-positron annihilation at LEP/SLC*, hep-ph9907500.

[37] A. Leike, T. Riemann, J. Rose, Phys. Lett. **B273** (1991) 513;
T. Riemann, Phys. Lett. **B293** (1992) 451;
S. Krisch, T. Riemann, Comp. Phys. Comm. **88** (1995) 89.

[38] The TOPAZ Collaboration (K. Miyabayashi *et al.*), Phys. Lett **B347** (1995) 171.

[39] The VENUS Collaboration (K. Yusa *et al.*), Phys. Lett. **B447** (1999) 167.

[40] ALEPH Coll. (D. Busculic *et al.*), Zeit. Phys. **C 71** (1996) 179.

[41] DELPHI Coll. (P. Abreu *et al.*), Eur. Phys. J. **C11** (1999) 383.

[42] L3 Coll. (M. Acciarri *et al.*), Phys. Let. **B 479** (2000) 101;
Determination of γ–Z interference in e^+e^- annihilation at LEP, CERN/EP-2000-084, subm. to Phys. Lett. **B**.

[43] OPAL Coll. (K.Ackerstaff et al.), Eur. Phys. J. **C2** *(1998) 441.*

[44] Reports of the working group on precision calculations for the Z resonance, eds. D. Bardin, W. Hollik and G. Passarino, CERN Yellow Report 95-03, Geneva, 31 March 1995, and references therein.